



HAL
open science

Simulating the net ecosystem CO₂ exchange and its components over winter wheat cultivation sites across a large climate gradient in Europe using the ORCHIDEE-STICS generic model

Nicolas Vuichard, Philippe Ciais, Nicolas Viovy, Longhui Li, Eric Ceschia, Martin Wattenbach, Christian Bernhofer, Carmen Emmel, Thomas Grünwald, Wilma Jans, et al.

► To cite this version:

Nicolas Vuichard, Philippe Ciais, Nicolas Viovy, Longhui Li, Eric Ceschia, et al.. Simulating the net ecosystem CO₂ exchange and its components over winter wheat cultivation sites across a large climate gradient in Europe using the ORCHIDEE-STICS generic model. *Agriculture, Ecosystems & Environment*, 2016, 226, pp.1-17. 10.1016/j.agee.2016.04.017 . hal-01587329

HAL Id: hal-01587329

<https://hal.science/hal-01587329>

Submitted on 23 Sep 2022

HAL is a multi-disciplinary open access archive for the deposit and dissemination of scientific research documents, whether they are published or not. The documents may come from teaching and research institutions in France or abroad, or from public or private research centers.

L'archive ouverte pluridisciplinaire **HAL**, est destinée au dépôt et à la diffusion de documents scientifiques de niveau recherche, publiés ou non, émanant des établissements d'enseignement et de recherche français ou étrangers, des laboratoires publics ou privés.



Distributed under a Creative Commons Attribution - NonCommercial 4.0 International License

Simulating the net ecosystem CO₂ exchange and its components over winter wheat cultivation sites across a large climate gradient in Europe using the ORCHIDEE-STICS generic model

Nicolas Vuichard^{a,*}, Philippe Ciais^a, Nicolas Viovy^a, Longhui Li^{a,b}, Eric Ceschia^c, Martin Wattenbach^d, Christian Bernhofer^e, Carmen Emmel^f, Thomas Grünwald^e, Wilma Jans^g, Benjamin Loubet^h, Xiuchen Wu^{a,i,j}

^aLaboratoire des Sciences du Climat et de l'Environnement (LSCE/IPSL), UMR 8212 (CEA/CNRS/UVSQ), 91191 Gif-sur-Yvette Cedex, France

^bPlant Functional Biology & Climate Change Cluster, University of Technology, Sydney, P.O. Box 123, Broadway, NSW 2007, Australia

^cCESBIO, UMR 5126 (CNES-CNRS-UPS-IRD), 18 avenue Edouard Belin, 31401 Toulouse Cedex 9, France

^dHelmholtz Centre Potsdam, German Research Centre for Geosciences GFZ, Telegrafenberg 14473, Potsdam, Germany

^eTechnische Universität (TU) Dresden, Institute of Hydrology and Meteorology, Chair of Meteorology, D-01062 Dresden, Germany

^fDepartment of Environmental Systems Science, Institute of Agricultural Sciences, ETH Zurich, 8092 Zurich, Switzerland

^gAlterra Wageningen University and Research, Wageningen, The Netherlands

^hUMR INRA-AgroParisTech, Environnement et Grandes Cultures, 78850 Thiverval-Grignon, France

ⁱKey State Laboratory of Land Surface Processes and Resource Ecology, Beijing Normal University, Beijing 100871, China

^jCollege of Resource Science and Technology, Beijing Normal University, Beijing 100875, China

Over the last decade, efforts have been carried on to develop and evaluate versions of global terrestrial ecosystem models (GTEM) in which crop specificities are represented. The goal of this study is to evaluate the ability of the ORCHIDEE-STICS (Organising Carbon and Hydrology In Dynamic Ecosystems—Simulateur multiDisciplinaire pour les Cultures Standard) GTEM in simulating the observed seasonal variations and annual budgets of net ecosystem exchange (NEE), gross primary production (GPP) and total ecosystem respiration (TER) fluxes over seven wheat sites spanning a large climate gradient in Europe. Overall, the seasonal variations of GPP are well represented by the model, with 5 sites out of 7 exhibiting a correlation coefficient (R) value higher than 0.9 and a normalized standard deviation (NSTD) between 0.8 and 1.2. In comparison, the model performances for catching the seasonal variations of TER are lower, especially in terms of NSTD. Regarding the annual budgets, mean simulated deviations averaged over all sites do not exceed 10% and 15% of the observed annual mean budget, for GPP and TER, respectively. For NEE, the model capacity at estimating annual budgets is low, its mean deviation corresponding to ~35% of the observed mean value. This clearly shows that more accurate model estimates of GPP and especially TER are required for estimating NEE annual budgets. In this respect, past land-use and land-management changes are probably the most crucial processes to add, for getting soil carbon disequilibrium and more accurate NEE annual budgets.

From a sensitivity analysis of the modelled fluxes to three management practices (plant variety, sowing date and fertilization intensity), we found that the fertilization is the most sensitive practice impacting the model performances of any flux, both in terms of seasonal variations and annual budgets.

1. Introduction

Croplands cover approximately 10% (Ellis and Ramankutty, 2008) of the terrestrial surface at global scale, and more than 30%

at European scale (Gervois et al., 2008). They consequently play a significant role within the global carbon cycle. The net ecosystem carbon balance (NECB, Chapin et al., 2006) at a cropland site is the sum¹ of gross primary production (GPP), total ecosystem respiration (TER) and lateral fluxes of carbon (C) (i.e. harvested C

* Corresponding author at: LSCE/IPSL, UMR CEA/CNRS/UVSQ 8212, CEA Saclay, Orme des Merisiers, Bât 712, 91191 Gif-sur-Yvette, France.

E-mail address: nicolas.vuichard@lscce.ipsl.fr (N. Vuichard).

¹ We use here the micrometeorological convention by which a flux is negative when the ecosystem is fixing carbon and positive when it is losing carbon.

consumed, C imported as seeds or tuber or manure and C displaced horizontally by erosion and either stored or decomposed into CO₂) which all respond to management and climate variability. Several studies found that the net ecosystem CO₂ exchange (NEE, sum of GPP and TER) of croplands results in a net atmospheric CO₂ sink on the order of 200 g C m⁻² yr⁻¹ (Ceschia et al., 2010; Kutsch et al., 2010; Moors et al., 2010; Loubet et al., 2011) while NECB is a net CO₂ source (Ceschia et al., 2010; Kutsch et al., 2010; Moors et al., 2010; Ciaïis et al., 2010; Bellamy et al., 2005; Smith et al., 2007; Loubet et al., 2011) of the order of 100 g C m⁻² yr⁻¹ when oxidation of harvested biomass was accounted for. Recently, Kindler et al. (2011) showed that dissolved organic carbon leaching losses were non negligible (of the order of 30 g C m⁻² yr⁻¹ for croplands), which could increase the strength of the NECB source. At the ecosystem scale, because there is no large litter input of C to the soil pools in these regularly harvested ecosystems, TER is lower than GPP, causing a larger negative NEE (sink). However, the site-to-site variability in carbon exchange is large and is determined by the choice of crop and practice, cultivation history, the location and to a lesser extent by the inter-annual variations in climate (Moors et al., 2010). Uncertainties on the carbon balance of croplands remain very large, in absence of systematic soil carbon inventories with revisit. The global terrestrial ecosystem models (GTEM) used for global and regional carbon cycle assessments (Canadell et al., 2011; Enting et al., 2012; Huntzinger et al., 2012) lack a description of croplands. Therefore, there is an increasing demand for GTEM to account for the interaction of human management and climatic effects in order to simulate a more realistic global carbon balance that considers the complexity of agricultural and especially arable systems.

Most of today's GTEM fail to model croplands functioning, in particular crop phenology and how carbon dynamics interacts with fertilization, irrigation, harvest and tillage practice. Recent efforts have led to a better representation of croplands within some GTEMs. This is the case for the ORCHIDEE-STICS model (de Noblet-Ducoudre et al., 2004; Gervois et al., 2004), the LPJmL model (Bondeau et al., 2007), the SIBcrop model (Lokupitiya et al., 2009), the Jules-sucros model (Van den Hoof et al., 2011), the ANTHRO-BGC model (Ma et al., 2011), the CESM1 model (Levis et al., 2012) or the CLM model (Billionis et al., 2015). New model developments for croplands need to be evaluated especially against site data like eddy-flux measurements. In addition, agricultural information such as the crop variety used, the sowing date or the fertilization practices are poorly known at regional to global scales. Consequently, it is of interest to investigate the sensitivity of the modelled fluxes to these management practices in order to prioritize further actions aiming at increasing the quality of management datasets.

Eddy-covariance is the state of the art technique for measuring the exchanges of energy, water and CO₂ between an ecosystem and the atmosphere, continuously, over long periods (from months to years) and at a scale representative of a crop field (from 0.01 to 4 km²) (Aubinet et al., 2000). Other micrometeorological techniques like the aerodynamic gradient method are more labour intensive and subject to potentially larger biases due to sampling line design and turbulence parameterisation (Loubet et al., 2013). Chamber measurements cannot deal easily with plot scales, although specially designed chambers exist for plant measurements (Pape et al., 2009). Paradoxically, even though the eddy flux technique was already employed in the late 70s/80s over crop ecosystems (Desjardins and Lemon, 1971, 1974; Anderson et al., 1984; Anderson and Verma, 1986; Ohtaki, 1984; Desjardins et al., 1984; Baldocchi, 2003), the first continental-scale eddy-covariance measurement networks were focused on forest ecosystems (Aubinet et al., 2000; Valentini et al., 2000; Running et al., 1999). In Europe, it was only during the CarboEurope-IP project (Schulze et al., 2009; www.carboeurope.org) that a network of 17 crop sites equipped with eddy-covariance

systems was established (Aubinet et al., 2009; Beziat et al., 2009; Kutsch et al., 2010; Ceschia et al., 2010).

In this study, we focus on the evaluation of the of the "Organising Carbon and Hydrology In Dynamic Ecosystems—Simulateur multiDisciplinaire pour les Cultures Standard" (ORCHIDEE-STICS) generic crop model. ORCHIDEE-STICS is a combined model (Gervois et al., 2004; de Noblet-Ducoudre et al., 2004) in which the process-based vegetation model (ORCHIDEE, Krinner et al., 2005) is chained to the STICS agronomical model (Brisson et al., 1998, 2002, 2003, 2008). STICS is run in this case to represent the phenology of cultivated plants and to account for farming practices. Daily foliar index (LAI) and nitrogen stress calculated by STICS are thus used to force ORCHIDEE, which calculates GPP and subsequent transformations of carbon assimilates (plant respiration, allocation, mortality and decomposition) according to its own equations. Currently, the chained model ORCHIDEE-STICS has been used for simulating wheat, soybean, maize and sugarcane (Smith et al., 2010a,b; Ciaïis et al., 2010; Vuichard et al., 2008; Valade et al., 2014). STICS has however sufficiently generic parameterizations to allow simulating also other crop species.

While having been evaluated against remotely-sensed leaf area index (LAI) (Smith et al., 2010a), national yield data (Smith et al., 2010b; Gervois et al., 2008; Vuichard et al., 2008), ORCHIDEE-STICS was compared with eddy covariance CO₂ flux data at only two North American crop sites (Bondville and Ponca, U.S.A. where are cultivated corn and wheat, respectively). Li et al. (2011) evaluated the same model simulating C flux (NEE) and latent heat fluxes at five European sites where maize was grown. Over these sites, the model simulations explained 75% of the variance of NEE. The model showed a better reproduction of measured GPP compared to TER variations. Based on sensitivity analyses, they concluded that any change in the intensity of each management practice considered in the study (fertilization, irrigation, crop calendar) changed the annual budget of NEE by more than 15%.

Currently, ORCHIDEE-STICS has only been tested at one wheat site, regarding its performance at simulating the seasonal LAI and C flux variations. Consequently, there is a need for better evaluating ORCHIDEE-STICS against CO₂ flux data across many sites where wheat is cultivated and under contrasted climatic conditions, a necessary condition for more realistic future spatially explicit applications.

The objectives of the study are:

1. To evaluate the capacity of the ORCHIDEE-STICS model to simulate the seasonal variations and annual budget of NEE and of its components (GPP and TER) over seven CarboEurope-IP wheat sites where carbon fluxes are monitored by eddy-covariance technique.
2. To identify for which component flux (GPP or TER) the model has largest errors and what are the mechanisms explaining model errors
3. To define the sensitivity of our simulation results with respect to changes in management parameters, in order to know what are the most critical management input data that need to be collected for making future regional applications on a grid.

2. Methods

2.1. Modelling-related information

2.1.1. Model description

2.1.1.1. STICS component. STICS is a 'generic' crop model that can be parameterized for many different crops (Brisson et al., 1998, 2002,

2003, 2008) and for specific varieties of a given crop. STICS is mainly applied at site-scale for agronomy applications. Crop phenology in STICS is subdivided in development stages that are sequentially simulated in the model. A thermal index (degree-day) adjusted for photoperiodic and vernalization effect defines the timing and duration of each stage and thus controls crop development. The calculation of the daily LAI growth rate (Δ_{lai} , $m^2 m^{-2} d^{-1}$) is expressed as a daily growth rate at the plant level expressed per degree-day ($\Delta_{lai,dev}$, $m^2 m^{-2} plant^{-1} (degree-day)^{-1}$) modulated by the effects of temperature (T , °C), plant density (f_{dens} , plants m^{-2}) and water and nitrogen limitations (f_W and f_N). Δ_{lai} is expressed by:

$$\Delta_{lai} = \Delta_{lai,dev} \times T \times f_{dens} \times \min(f_W f_N) \quad (1)$$

$\Delta_{lai,dev}$ is a function of the development stage unit and follows a logistic function. f_W is a linear function of the available water content (water content above the wilting point, $m^3 m^{-3}$) in the root zone, that equals one when the water content is higher than 0.2. f_N is a function of the C/N ratio in the plant (CN_{plant}) and is written as:

$$f_N = \max(\min(-0.8 + 1.8 \times CN_{plant}/CN_{crit}, 1), f_{N,max}) \quad (2)$$

where CN_{crit} is a critical C/N ratio function of the total biomass and $f_{N,max}$ a maximal nitrogen stress index which equals to 0.3 (Brisson et al., 2008).

The development stages and the thermal requirement between two consecutive stages are defined in STICS for three varieties of wheat (Talent, Thesee, Arminda) that we use in our study. These variety-specific parameterizations are summarized in Appendix A.

2.1.1.2. ORCHIDEE component. The ORCHIDEE model (Krinner et al., 2005) calculates CO_2 , H_2O and heat fluxes, for diverse vegetation types (plant functional types, PFTs) at scales going from point to global gridded simulations. This model is mainly applied for carbon budgeting and carbon cycle applications. It contains a biophysical module calculating photosynthesis, water and energy balance calculations on a 30-min basis, and a carbon dynamics module dealing with phenology, growth, allocation, mortality and soil organic matter decomposition, on a daily basis. Carbon exported via leaching/imported from organic manure is not accounted for in ORCHIDEE.

Carbon assimilation by photosynthesis is done per canopy layer, based on the formulas developed by Farquhar et al. (1980) and Collatz et al. (1992) for C3 and C4 species, respectively. It is coupled to the transpiration via the stomatal conductance calculation, following the formulation of Ball et al. (1987). The nitrogen stress index (f_N) calculated in STICS directly impacts the values of the maximum rate of Rubisco activity-limited carboxylation ($V_{c,max}$, $\mu mol CO_2 m^{-2} s^{-1}$) and the maximum rate of electron transport under saturated light (J_{max} , $\mu mol e-m^{-2} s^{-1}$). Integration of the assimilation along the canopy (GPP) uses the LAI calculated in STICS and accounts for radiation extinction using the Beer-Lambert's law (Monsi and Sæki, 1953). In ORCHIDEE (Krinner et al., 2005), the autotrophic respiration (AR) is decomposed in two terms: the maintenance respiration (MR) and the growth respiration (GR). MR is proportional to the size of the living biomass pools and modulated by a temperature function, which linearly increases with temperature. A fixed fraction (28%) of the remaining allocatable biomass (GPP-MR) corresponds to GR. The heterotrophic respiration (HR) is calculated according to the Century model developed by Parton et al. (1988). In Century, the organic matter (OM) is stored in different pools, the time of residence of the organic matter in a pool being proportional to its resistance to decomposition. In ORCHIDEE-STICS, the time of residence of the OM in arable soils is set to 70% of its value for natural lands. Dead biomass goes into 4 litter pools for above and

below ground OM and structural (slowly decomposing) and metabolic (quickly decomposing) biomass. Soil carbon, resulting from litter decomposition, is present in three different pools: active, passive, and slow. Flows of carbon from one pool to another are modulated by soil temperature and humidity functions and are associated with different CO_2 losses by respiration. HR is calculated as the sum of these CO_2 losses.

NEE is then calculated as:

$$NEE = GPP + AR + HR \quad (3)$$

By convention, one assumes that sources of CO_2 to the atmosphere are positive and consequently GPP has negative sign in Eq. (3). However, in the following, GPP will be expressed with opposite sign, with positive values.

2.1.2. Simulations set-up

The ORCHIDEE-STICS model was driven at each site by observed gap-filled hourly temperature, precipitation, downward longwave and shortwave radiation, relative humidity and wind speed. The soil water holding capacity parameters (wilting point and field capacity) are derived from the texture of the site based on the work of Jamagne et al. (1977) as proposed in Brisson et al. (2008).

Before analysing the ORCHIDEE-STICS output over the period of measurements, we perform a 1000-year spin-up simulation during which climate, CO_2 atmospheric concentration and management practices of the studied year are repeatedly cycled. A long spin-up is necessary for the soil carbon pools that have a long residence time. The carbon, nitrogen and water pools are then initialized with the steady-state values obtained at the end of the spin-up simulation. In the control simulation (CTRL), management events of fertilization, sowing, harvest and ploughing used to drive ORCHIDEE-STICS are based on on-site observed values. Because the varieties of wheat cultivated were different at the seven sites and the variety-related parameters of STICS are unknown for all these varieties, we arbitrarily used the set of agronomical parameters associated to the 'Arminda' variety for running the CTRL simulation (see Table A1 in Appendix A).

In addition to the CTRL simulation, we performed six sensitivity simulations (3 types of practices under 2 different scenarios), in order to compare the sensitivity of simulated CO_2 fluxes to different types of management input data. These simulations differ from the CTRL simulation by varying one at a time the plant variety (2 simulations with two different varieties than Arminda), the sowing date (2 simulations with advanced and delayed sowing) and the amount of N-fertilizer applied (2 simulations with no and high N input). The model simulations plan with the name of each sensitivity test is given in Table 2. In the simulations called LOPLANT and HIPLANT, the sowing date is varied with seeds planted respectively 25 days earlier and later than in the CTRL simulation ($\pm 2\sigma$ of the observed sowing dates distribution at the 7 sites). In the NOFERT simulation, no fertilization is considered while in the HIFERT simulation, an automated nitrogen (N) fertilization of $50 kg N ha^{-1} day^{-1}$ every time the plants become N-limited in the STICS simulation is applied. To simulate different wheat varieties, we use the set of agronomical parameters defined in STICS corresponding to 'Talent' and 'Thesee' varieties, alternatively to the 'Arminda' variety (details on the STICS parameters varying between varieties are given in Appendix A).

2.2. Observation-related information

2.2.1. Sites description

Over the time period of the CarboEurope-IP project (2003–2007), wheat was grown at least one year at 10 out of 17 European cropland sites. Among the 10 sites, we selected a subset of 7 years

for which the meteorological and CO₂ fluxes data were sufficient for running and/or evaluating ORCHIDEE-STICS, which leads to seven site-years. These site-years are Auradé (AUR, France in 2005–2006), Lamasquère (LAM, France in 2006–2007), Grignon (GRI, France in 2005–2006), Klingenberg (KLI, Germany in 2005–2006), Gebesee (GEB, Germany in 2006–2007), Oensingen (OEN, Switzerland in 2006–2007) and Lutjewad (LUT, The Netherlands in 2006–2007). The sites are located across Europe along a SW-NE transect (Fig. 1). The mean annual air temperature at these sites ranges from 6.8 to 13 °C (KLI and AUR, respectively) and annual precipitation from 490 to 1585 mm (GRI and OEN, respectively).

2.2.1.1. Auradé. The Auradé site (AUR) is located in the South of France (43°33'N–01°06'E) at 240 m elevation. Soil texture at the site location is clay loam. The cropping system at this site is a winter wheat–sunflower–rapeseed rotation, initiated approximately in 2000. At AUR, only grains are exported, the straw being let on the ground at harvest. During the studied crop season (2005–2006), the mean annual air temperature was 13 °C and annual precipitation 684 mm.

2.2.1.2. Lamasquère. The Lamasquère site (LAM) is located in the South of France (43°30'N–01°14'E). The site is at 180 m elevation and soil texture is clay loam. Since 2000, the site has been used for cultivating maize for silage and winter wheat. At harvest, both the grain and the straws were exported. During the crop season 2006–2007 when wheat was grown, the mean annual air temperature was 13 °C and annual precipitation 620 mm.

2.2.1.3. Grignon. The Grignon site (GRI) is located in France near Paris (48°9'N–01°95'E) at 125 m elevation height. The soil type is classified as luvisol over loess. The site was managed with maize–winter wheat–barley rotation; while mustard was used for some intercrop periods before maize. During the study crop season (2005–2006), the mean annual air temperature was 10.9 °C and the annual precipitation 490 mm. Details of the site are given in Loubet et al. (2011).

2.2.1.4. Klingenberg. The Klingenberg site (KLI) is located in the East of Germany (50°54'N–13°31'E) at 480 m elevation height. It has a pseudogley soil. Winter barley, rapeseed, winter wheat, maize and spring barley were cultivated at this site. We focus here on the crop season 2005–2006 during which winter wheat was

grown. During this period, the mean annual air temperature was 6.8 °C and the annual precipitation amounted 607 mm.

2.2.1.5. Gebesee. The Gebesee site (GEB) is located in the Center of Germany (51°06'N–10°55'E) at 165 m elevation height over a rich loess soil. It was used for cultivating winter wheat, potatoes, rapeseed and barley. The crop season studied is 2006–2007 during which mean annual air temperature was 11.1 °C and annual precipitation was 648 mm.

2.2.1.6. Oensingen. The Oensingen site (OEN) is located in Switzerland (47°17'N–7°43'E) at 452 m elevation height. The soil is classified as silty clay. The crop rotation at this site included rapeseed, winter wheat, barley and potatoes. Mean annual air temperature was 11.5 °C and annual precipitation was 1525 mm during the study crop season (2006–2007).

2.2.1.7. Lutjewad. The Lutjewad site (LUT) is located in the North of the Netherlands (53°24'N–6°21'E) at sea level. The soil is classified as Calcaric epigleyic Fluvisol. During the 2000s, only winter wheat has been cultivated at LUT but C fluxes and meteorological variables were only monitored in 2006 and 2007. Consequently the season 2006–2007 was the unique full crop period during the monitoring period. During that crop season, the mean annual temperature was 11.6 °C and annual precipitation amounted to 1094 mm.

2.2.2. Observations used for running or evaluating the model

2.2.2.1. Micrometeorological measurements. Micrometeorological measurements were made at every site on at least a half-hourly basis. They included air temperature, air relative humidity, wind speed, incoming short- and long-wave radiation, atmospheric pressure and precipitation. In-situ micrometeorological measurements were used as inputs for running the ORCHIDEE-STICS model at site level. Instrumental characteristics (height, sensors types) are summarized in Table B1 of Appendix B.

2.2.2.2. Management information. At AUR, the seeds were planted on the 27th of October 2005 and the harvest occurred on the 29th of June 2006. Mineral fertilizer was applied successively in January, March and April 2006 for a total amount of 123.5 kg N ha⁻¹. On the 30th of September 2006 the soil was ploughed. At LAM, the sowing date was 18th of October 2006 and the harvest date was 15th of July

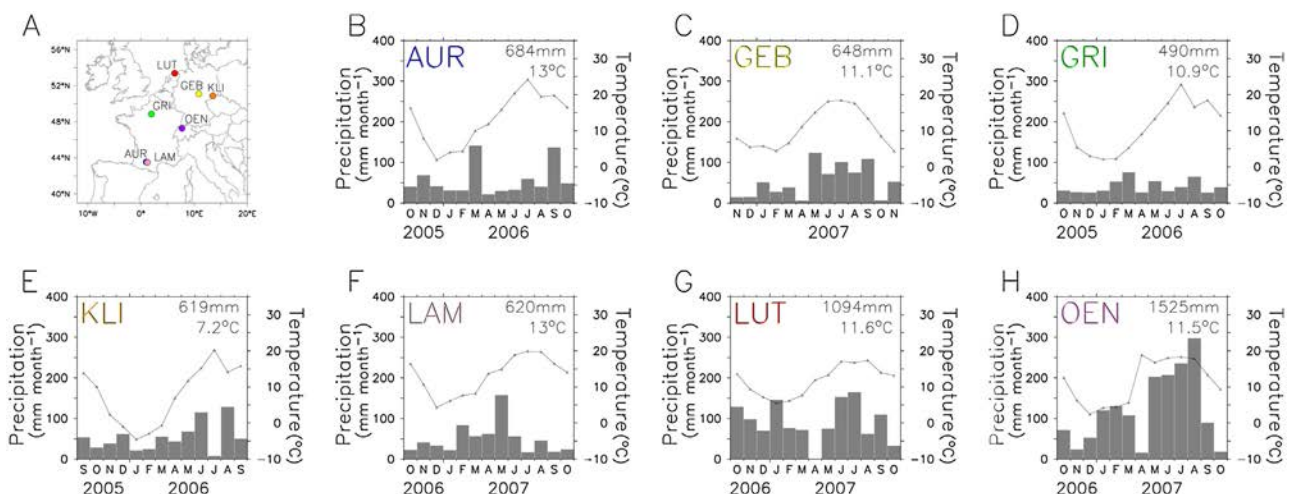


Fig. 1. (A) Location, (B–H) mean air temperature (°C) and total precipitation (mm) at both annual (numbers in top right corners) and monthly time-step (solid lines and grey bars, respectively) for the seven sites over the studied one-year period starting on the sowing dates.

2007. Two applications of mineral fertilizers were performed (January and April 2007) with a total amount of 95 kg N ha^{-1} . In October 2006, solid and liquid organic manure were applied (30 t ha^{-1} and 50 t ha^{-1} , respectively). At GRI, the sowing and harvest dates in the period studied are 28th of October 2005 and 15th of July 2006, respectively. During that period, the site received mineral fertilizers (nitrogen solution) in two applications (in March and April 2006) of 55 kg N ha^{-1} each. At KLI, the seeding occurred on 25th of September 2005 and the crop was harvested on 6th of September 2006. Between these two events, four applications of mineral fertilizers occurred (in April, May and June) for a total amount of $\sim 200 \text{ kg N ha}^{-1}$. At GEB, sowing occurred in November 2006 and harvest in early August 2007. During this period, 110 kg N ha^{-1} were applied to the site, among which $\sim 20 \text{ kg N}$ as manure. At OEN, the sowing and harvest dates were 19th of October 2006 and 16th of July 2007, respectively. During this period, three fertilizing events occurred (in March, April and May 2007) providing a total amount of 140 kg N ha^{-1} . At LUT, the sowing occurred in October 2006 and the harvest in early August 2007. During that period, $\sim 200 \text{ kg N ha}^{-1}$ were applied, split into three applications (March, April and May).

2.2.2.3. Leaf area index and above ground biomass measurements. At all sites (except GEB), leaf area index (LAI) was either measured with a non-destructive method, on the basis of randomly spatially distributed plants by means of a LI-COR planimeter (LI-3100, LI-COR, Lincoln, NE, USA), or with a destructive method by sampling a set of plants, measuring a subset of plants surfaces and upscaling based on the plant biomass. In addition, above ground biomass (AGB) was also measured at four of the seven sites (AUR, KLI, GRI and LAM). Between 4 and 10 measurements of LAI and AGB were done over the crop season, depending on the site.

2.2.2.4. NEE measurements. Measurements of NEE using the eddy covariance technique were done at each site, based on continuous high-frequency measurements of the three components of wind velocity, CO_2 concentration and water vapour density. They are carried out with a set of instruments including a 3-D ultrasonic anemometer and an open- or closed-path infrared gas analyzer (IRGA) mounted on the top of a $\sim 2\text{--}3 \text{ m}$ tower (see Table B1 in Appendix B for more detail on instruments specificities at each site). NEE was calculated as the covariance of the vertical component of the wind velocity and the molar ratio of CO_2 in dry air. A correction to account for variations in air density due to water vapour and temperature was applied (the Webb Pearman Leuning correction, Webb et al., 1980) when using an open-path IRGA. In order to ensure that the flux footprint was representative of the studied plot and not of a nearby plot, a footprint analysis was performed and raw flux data removed when needed. More information on instrumental set-up, acquisition mode and data processing techniques are described in Aubinet et al. (2000), Dolman et al. (2006) and Reichstein et al. (2005).

2.2.3. Treatments done after data acquisition

2.2.3.1. NEE gap-filling procedure. Gaps in the NEE time-series acquired at site-level can be due to missing data (because of instruments maintenance and calibration, power outages or blockage of the system) and rejection of bad quality data (related to interference of water condensation and rain drops with the optical path of the IRGA, or fluxes associated to low turbulence conditions). The gap-filling of NEE was performed applying the marginal distribution sampling (MDS) method (Reichstein et al., 2005). Hereby, given the fact that meteorological data were available without gaps, missing values

of NEE were replaced by average values under similar meteorological conditions within a time window of ± 7 days. Similar meteorological conditions correspond to time periods when global radiation (R_g), air temperature and vapour pressure deficit do not deviate from each other by more than 50 W m^{-2} , $2.5 \text{ }^\circ\text{C}$ and 5.0 hPa , respectively. If for a gap, no similar conditions were available, the averaging window was increased to ± 14 days and similar conditions were defined only based on R_g or simply the measurement time (see Reichstein et al., 2005 for details). An uncertainty of between 4% and 6% is expected due to gap-filling procedure (Beziat et al., 2009; Ammann et al., 2009). The percentage of gap-filled half hourly data exceeds 50% on an annual basis at two sites (LAM and OEN) over the seven studied sites but more than 90% of the NEE data at any site were classified as “original value” (quality class 0) or “most reliable gap-filled” (quality class 1) (Sus et al., 2010).

2.2.3.2. NEE partitioning into gross fluxes. The partitioning of NEE into GPP and TER fluxes was obtained from the CarboEurope-IP data portal. TER was separated from NEE applying the algorithm of Reichstein et al. (2005) that derives a short-term temperature sensitivity of TER from night-time eddy covariance CO_2 fluxes based on an exponential regression model (Lloyd and Taylor, 1994):

$$\text{TER} = \text{TER}_{\text{ref}} e^{E_0(1/(T_{\text{ref}}-T_0)-1)/(T-T_0)} \quad (4)$$

Regressions were performed for sub-periods of 15 days, with consecutive time windows overlapping 10 days, in order to estimate the temperature sensitivity parameter E_0 , setting the reference temperature (T_{ref}) to $10 \text{ }^\circ\text{C}$ and keeping constant the parameter T_0 at $-46.02 \text{ }^\circ\text{C}$ as in Lloyd and Taylor (1994). The temperature independent base respiration rate (TER_{ref}) was then estimated for consecutive 4-day periods by non-linear regression using Eq. (4) fixing all parameters except TER_{ref} . To produce a continuous time serie, TER_{ref} estimates were then linearly interpolated.

Desai et al. (2008) evaluated 23 different methods to separate GPP and TER from NEE, including the one developed by Reichstein et al. (2005) over 10 site-years. They evaluate the ability of the GPP and TER flux partitioning methods to retrieve GPP and TER from synthetic data. In particular, they looked at the annual bias between modelled GPP (resp. TER) and ‘true’ GPP (resp. TER) and at the correlation between daily modelled and ‘true’ GPP (resp. TER). They showed that the Reichstein et al. method was one of the techniques with the best performance for both bias and correlation. Across the 10 site-years, the Reichstein et al. method was biased low against the ‘true’ annual GPP and TER but this bias never exceeded 5% of the annual ‘true’ value. This error is low compared to the errors (model-data misfits) associated with the fluxes modelled by ORCHIDEE-STICS. Consequently, we consider that GPP and TER estimates based on the Reichstein et al. (2005) method can be used as observation-based products suitable to evaluate the modelled GPP and TER.

The period between sowing and the start of photosynthetic activity (defined as the appearance of the first diurnal cycle in GPP with an amplitude equals to 5% of maximum seasonal amplitude) ranges from 3.5 months at LAM to 6 months at KLI. Klingenberg is the site where seeds are planted the earliest (end of September, see Table 1). The growing season length (defined as the period between the start of the photosynthetic activity and the harvest), ranges from 3.5 months at AUR to 5 months at GEB. During the growing season, maximum daily assimilation varies among sites from 14 to $24 \text{ g C m}^{-2} \text{ d}^{-1}$ both in model and data.

2.3. Metrics for model evaluation

For LAI, we evaluate the model error by mean of the root mean square error (RMSE). We also used the figure of merit (FMT), defined by the area under union of the two curves of modelled and observed LAI divided by the area defined by their intersection. FMT is written as:

$$FMT = \frac{\sum_{j=1}^n \min(obs_j, mod_j)}{\sum_{j=1}^n \max(obs_j, mod_j)} \quad (5)$$

where n is the number of data points and obs and mod , the observed and modelled LAI values, respectively.

A value of FMT close to 1 means a perfect agreement between model and observations opposed to a value of FMT close to 0 meaning no match between both data sets.

The assessment of the model performance in simulating the observed seasonal variations of GPP, TER and NEE fluxes is based on the comparison of the observed and modelled daily fluxes. We analyse the three components of the model/data misfit proposed by Kobayashi and Salam (2000), the first one characterizing the mean bias, the second one characterizing the error on structure and phase (or correlation) and the third one characterizing the error in the amplitude of the variations (or standard deviations). The correlation with the daily observations (R-value, component 2) and the standard deviation (normalized to the standard deviation of the observations, NSTD, component 3) are represented by the mean of Taylor diagrams (Taylor, 2001). In such diagrams, the model's performance of each site is represented by a single point, indicating the R-value along the polar angle, and the NSTD along the polar axis: The closer to 1 the R-value and the NSTD are, the better the agreement between model and observation is. When analysing the model/data misfit at seasonal scale, we calculate at each site the one-month critical period defined as the one-month period for which the mean absolute deviation of the modelled flux to the observed flux is the largest.

When presenting the sensitivity of the seasonal flux variations to management practices, we also use Taylor diagrams with arrows, where the start of the arrow corresponds to the CTRL

simulation and the end to the sensitivity simulation. In these diagrams, the longer the distance is between the two simulation points, the more sensitive is the flux to the considered management practice.

We also compare modelled and observed budget of GPP (GPP_{cum}), TER (TER_{cum}) and NEE (NEE_{cum}), on an annual basis, starting from the sowing date. This quantifies the mean bias of the modelled estimates (component 1). When comparing annual fluxes, we group all the sites together and quantify the RMSE of the modelled annual budget to the observed one. At each site, we also quantify the error percentage (EP) that is defined as the ratio of the difference between the observed and modelled values to the observed value.

3. Results and discussion

3.1. Seasonality

3.1.1. LAI and AGB

The model performance in simulating the seasonal dynamic of LAI varied across sites (Fig. 2). The modelled LAI matched well the amplitude and phase of the observations only at OEN (RMSE = 0.6 $m^2 m^{-2}$ and FMT = 0.8) and to a lesser extent at KLI (RMSE = 1.0 $m^2 m^{-2}$ and FMT = 0.6). However, one should note that there is no LAI data at OEN after the beginning of May. Note also that modelled LAI is not directly comparable to observations, ORCHIDEE-STICS representing only green LAI while total LAI is measured at site. At AUR, LAM and GRI, modelled crop emergence was delayed by a week to a month, which led to a FMT value of 0.4 for these three sites. In addition, modelled maximal LAI over the growing season was overestimated at AUR and LAM by up to 4 $m^2 m^{-2}$ (Fig. 2), which translated into the highest RMSE values ($\sim 2.8 m^2 m^{-2}$). At LUT, modelled maximal LAI was also overestimated by up to 2 $m^2 m^{-2}$. At GEB, albeit no LAI measurement was available, the modelled maximal LAI was rather low (of the order of 2 $m^2 m^{-2}$) compared to the other sites. Compared to LAI, the model performed better at simulating the dynamic of AGB. In particular, the timing of the growth stage was better reproduced. The amplitude of the AGB dynamics was well simulated by ORCHIDEE-

Table 1
Management-related information of the seven sites during the one-year studied where Min and Org stand for mineral and organic fertilizer, respectively.

Site/unit	Sowing dd/mm/yy	Harvest dd/mm/yy	Ploughing dd/mm/yy	Fertiliser application dd/mm/yy	Fertiliser type -	Amount N (kg N ha ⁻¹)
AUR	27/10/05	29/06/06	30/09/06	25/01/06	Min	50.0
				23/03/06	Min	40.0
				12/04/06	Min	33.5
GEB	09/11/06	07/08/07	30/08/07	11/04/07	Org	~20
				03/05/07	Min	90.8
GRI	28/10/05	15/07/06	28/10/05	15/03/06	Min	55.0
			04/10/06	14/04/06	Min	55.0
KLI	25/09/05	06/09/06	23/09/05	08/04/06	Min	74.2
				04/05/06	Min	53.8
				04/06/06	Min	35.8
				22/06/06	Min	43.1
LAM	18/10/06	15/07/07	none	18/01/07	Min	46.5
				05/04/07	Min	48.2
LUT	20/10/06	04/08/07	10/10/06	14/03/07	Min	104.0
			01/10/07	30/04/07	Min	57.2
				04/05/07	Min	26
OEN	19/10/06	16/07/07	17/10/07	15/03/07	Min	50.0
				17/04/07	Min	40.0
				27/05/07	Min	50.0

Table 2

Summary of the simulation set-up for the control simulation and the model sensitivity tests. OBS indicates that at each site, sowing date or fertilization is prescribed to the model from the observation at each site.

Simulation name	Sowing date			Fertilization			Variety		
	25 days earlier	OBS	25 days later	none	OBS	maximal	Talent	Arminda	Thésé
CTRL		×			×			×	
LOPLANT	×				×			×	
HIPLANT			×		×			×	
NOFERT		×		×				×	
HIFERT		×				×		×	
VTA		×			×		×		
VTH		×			×				×

STICS over two (KLI and LAM) of the four sites where AGB was measured, but was significantly underestimated at the two other sites (AUR and GRI).

3.1.2. GPP

Overall, the seasonal variations of GPP were well represented by the model (left column of Fig. 3). This is especially true when considering inter-site differences.

At AUR, LAM and GRI, the modelled onset of GPP was delayed by on average 2 weeks compared to observations. This is likely due to the STICS model simulating a too late crop emergence at these sites (see Fig. 2). On the opposite, KLI exhibited a delay of approximately one month for the crop emergence, and yet a good match for the GPP onset (Fig. 3). At the LAM site, Beziat et al. (2009) mentioned that GPP in spring 2007 started early due to abnormally warm temperatures during the former winter. This early GPP onset was not reproduced by the model, which suggests model error in the formulation or the parameterization of the vernalisation mechanisms (e.g. seed development response to temperature in STICS). Modelled maximal LAI over the growing season was overestimated at AUR, LAM and LUT by up to $4 \text{ m}^2 \text{ m}^{-2}$ (Fig. 2), but this bias did not translate into a parallel overestimation of the GPP, excepted at LAM. This shows that GPP is less sensitive to LAI when it is relatively high, due to the fraction of absorbed radiation which is expressed as $1 - \exp(-0.5 \times \text{LAI})$. This shows also that there are other factors impacting the canopy photosynthetic rate that may compensate for the possible positive GPP bias induced by too high LAI. However, the reason why AUR and LAM respond differently in terms of GPP to a similar LAI positive bias at the end of the growing season remains unclear, but could be explained by the strong water deficit experienced at AUR in May/June 2006 that negatively impacts on GPP and to which the model might be too sensitive.

LUT exhibited an opposite behaviour to AUR, LAM and GRI, with an early bias of modelled GPP in spring. This GPP bias was not explained by an LAI bias of the same sign (compare Figs. 2 and 3). For three sites among the four at which there was a modelled GPP early-bias at the start or in the end of the growing season (AUR, LAM, LUT), this model/data mismatch during the early and late growing season period corresponds to the one-month critical period (area shaded in grey in Fig. 3).

At the four other sites, we identified the one-month critical periods in April 2007 at the OEN and GEB sites (model underestimation of GPP), from mid May to mid June 2006 for KLI (model overestimation of GPP) and in May 2006 for GRI (model overestimation of GPP). All these critical periods occur in the middle of the growing season. For GRI, the GPP model overestimation is probably due to a too high LAI value as an indirect consequence of the late modelled crop emergence (observed maximal LAI value occurred in early May and simulated one is delayed by one month).

For OEN and GEB, there was a large precipitation deficit in April 2007 (see Fig. 1). The model likely overestimated the effect of this

spring drought on GPP, in view of the low simulated GPP values. On the opposite, at KLI, the GPP model overestimation relates to insufficient water stress consecutive to a rainy period during March–April 2006. This shows that model shortcomings occur during critical periods associated with large soil moisture changes, hence the need of representing soil moisture profiles and root uptake of water from different soil depth. Our results indicate that the ORCHIDEE-STICS soil model has a too short water residence time in the root zone, causing an over-sensitivity of GPP to both rainfall deficit and excess. Overall, the dynamic of the latent heat flux over the growing season (see Fig. D1 in Appendix D) followed the one of the GPP, which shows the strong link between carbon and water fluxes via the stomatal conductance. In particular, the latent heat flux was strongly overestimated by the model at LAM in June 2007 as it was for GPP. Note, however the rather strong model/data disagreement for the latent heat flux at OEN, where the model did not underperform at simulating GPP compared to other sites.

Although all the one-month long critical periods of large model-data misfits occurred during the growing season (between sowing and harvest), model/data differences were also significant outside of the growing season. This was notably the case after the harvest: in ORCHIDEE-STICS, there is no more assimilation (LAI equals zero) while in reality, re-growth (volunteer or not) induces GPP (see for instance AUR, GRI or OEN sites in Fig. 3) as observed by Aubinet et al. (2009) and Beziat et al. (2009).

In order to summarize the performances of different model simulations, the Taylor diagrams (Taylor, 2001) that provide a graphic representation of the model/data correlation coefficient (R) and of the normalized Standard Deviation (NSTD) are shown in Fig. 4. The R-values of daily GPP were always higher than 0.8, with 5 sites out of 7 exhibiting an R-value higher than 0.9. These R-values were higher than those reported by Li et al. (2011) over maize sites (R-values range from 0.56 to 0.90). Observed GPP day-to-day amplitude was also well reproduced by the model, the distance between model and data NSTD generally not exceeding 0.2 except for two sites (KLI and LAM, 0.23 and 0.56 respectively).

3.1.3. TER

In comparison of those obtained for GPP, model/data correlations for TER were lower: R-value was higher than 0.9 at 3 sites only (GEB, KLI and GRI, see Fig. 4). However, the most noticeable change was the model NSTD spread along the best value (NSTD=1). The absolute difference between the model NSTD and the observation NSTD was up to 0.2 for four sites. The lower model performance in representing TER variations, compared to GPP, was also observed by Li et al. (2011) over sites where maize was grown.

AR is coupled to GPP and contributes the most to TER during the growing period. Consequently it is not surprising to note some covariance between TER and GPP seasonal variations. The correlation coefficient between observed GPP and TER was high (R-values range from 0.78 (GRI) to 0.93 (LUT)) and similar R-values

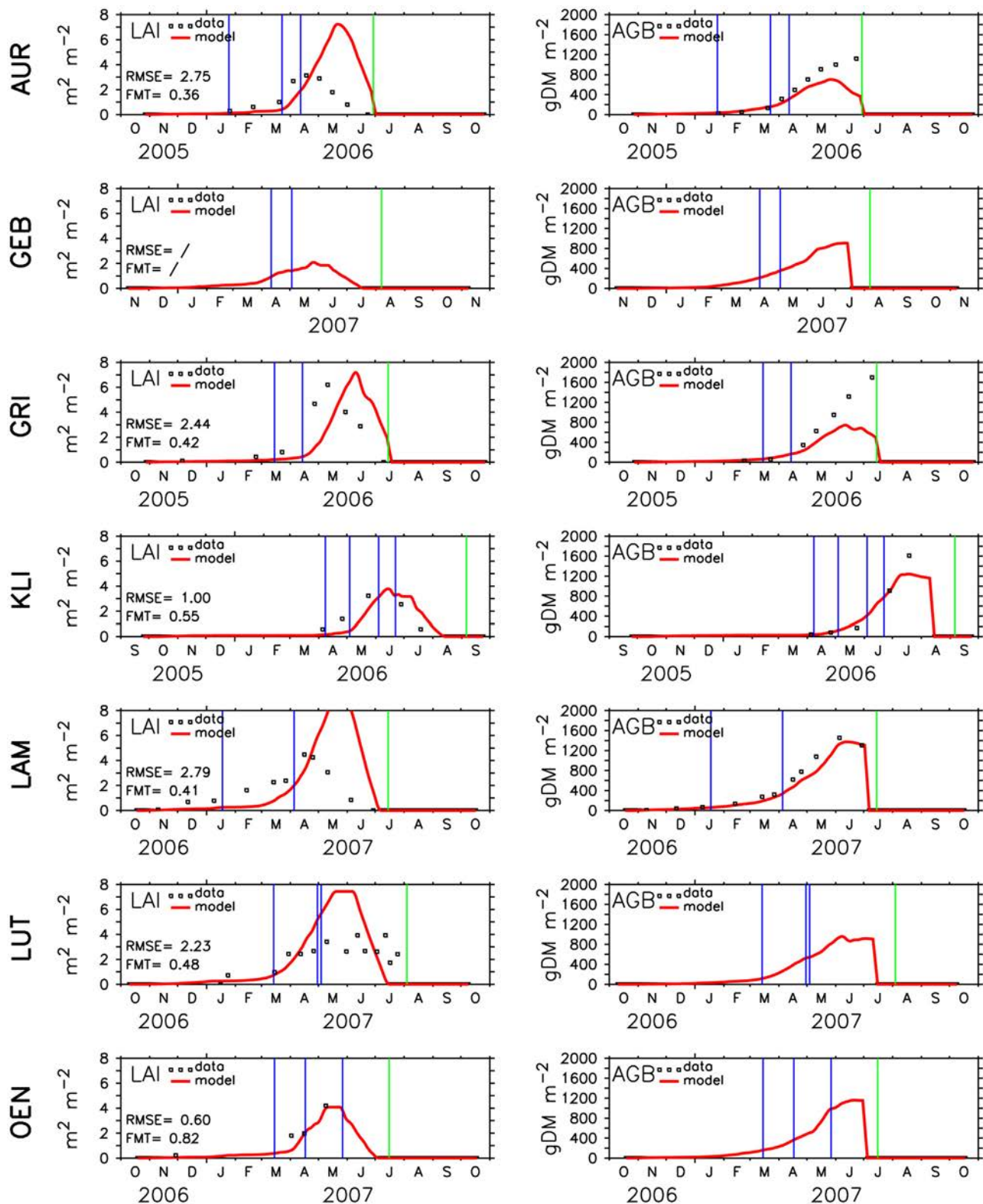


Fig. 2. Observed and modelled Leaf Area Index ($\text{m}^2 \text{m}^{-2}$) and aboveground biomass (AGB, gDM m^{-2}) for the seven sites over the studied one-year period starting on the sowing date. The blue and green lines indicate fertilization events and harvest dates, respectively. (For interpretation of the references to colour in this figure legend, the reader is referred to the web version of this article.)

were obtained with the modelled fluxes. Overall, the mean modelled AR to GPP ratio averaged over the 7 sites equalled 0.4. It is quite comparable with in-situ estimates that range from 0.3 and 0.6 (Amthor, 2000a; Cannell and Thornley, 2000; Thornley and Cannell, 2000; Aubinet et al., 2008). Thus, some of the model/data

mismatches for TER may be directly attributed to GPP mismatches. This was the case at LAM in June 2007 or at LUT from mid-May to mid-June 2007 (middle column of Fig. 3). The one-month critical periods associated to large model-data misfits of GPP and TER coincided exactly only at GRI and LAM, leading to the hypothesis

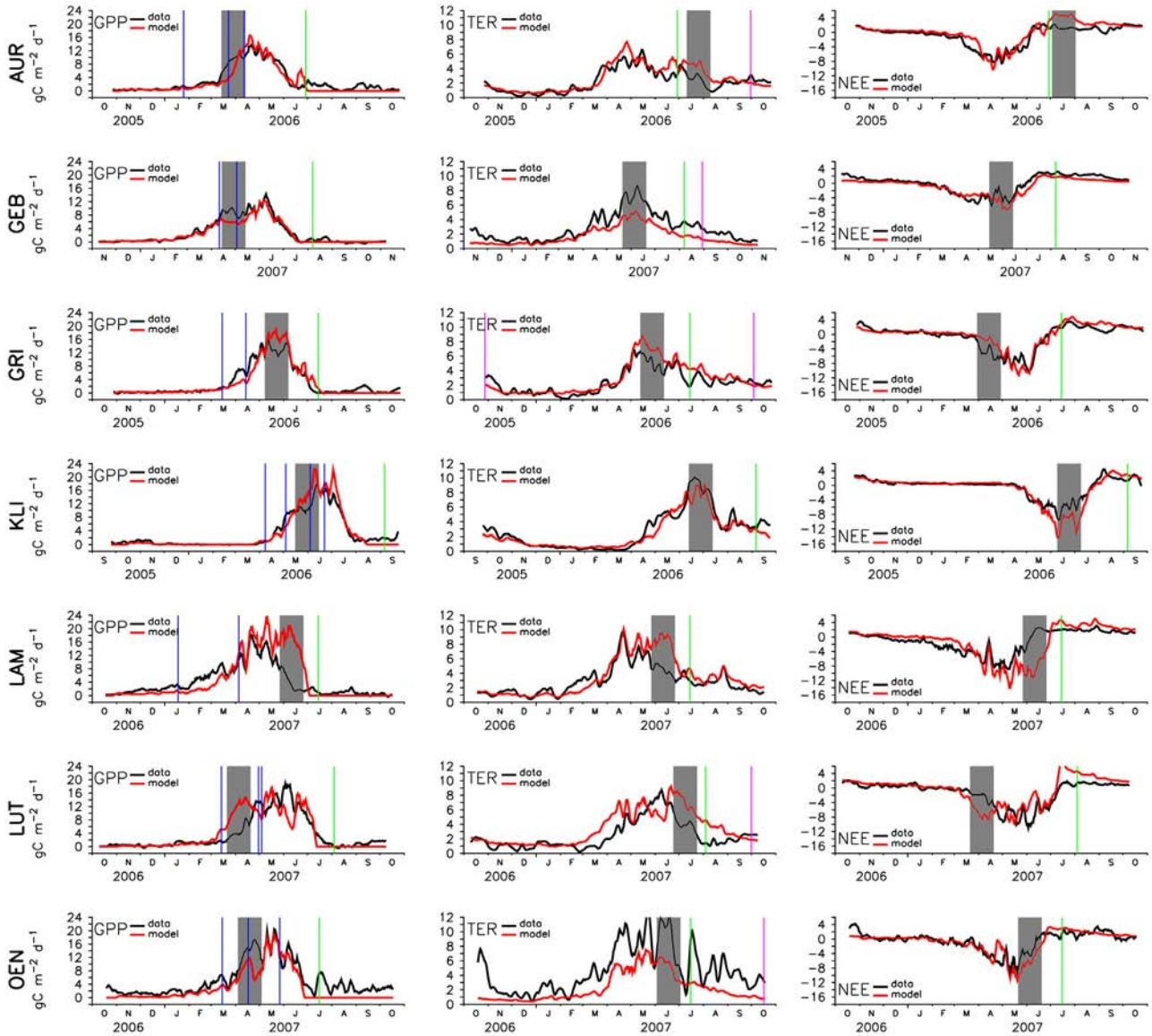


Fig. 3. Observation-based (black) and modelled (red) daily variations (five days running mean) of GPP (left panels), TER (middle panels) and NEE (right panels) expressed as $\text{gC m}^{-2} \text{d}^{-1}$ for the seven studied sites over a one-year period starting on the sowing dates. Grey shaded band represents the one-month critical period defined as the one-month period for which the mean absolute deviation of the modelled flux to the observed flux is the largest. The blue, pink and green lines indicate fertilization events, ploughing events and harvest dates, respectively.

that there are other TER specific mechanisms that explain the discrepancies with the data at other sites. For three sites, the one-month critical period of high TER model-data misfit occurred once biomass was senescent before (OEN and LUT) or just after harvest (AUR). For AUR and LUT, this period corresponded to a model overestimation of TER. This suggests that litter is too quickly decomposed in ORCHIDEE-STICS. On the opposite, for OEN, the critical period was associated with a model underestimation of TER in June 2007 (Fig. 3). In fact, the observed TER at OEN was very specific: the maximal value was up to $12 \text{ gC m}^{-2} \text{d}^{-1}$ and the intra-seasonal variations were much more abrupt than for the other sites. For this site in particular, NEE partitioning has been performed additionally with another methodology (Lasslop et al., 2010), independent of the one used in the present study

(Reichstein et al., 2005). Temporal dynamics of GPP and TER resulted in similar patterns than those obtained with the Reichstein et al. methodology, indicating that the observed-based TER and GPP dynamics are rather robust.

The assignment of the model error on TER to AR or HR is challenging. At GEB, the positive TER values in the observations in November 2006 or in September 2007 when GPP is zero and vegetation absent indicate a model TER error related to HR. In that case, the process is a too slow soil carbon and litter decomposition response to climate (or too small soil carbon stocks) in the model. At OEN, the model/data misfit might be related to an error in simulating AR, because the TER variations closely correlated to those of GPP (Fig. 3). This bias may be explained by a variety-specific GPP to AR ratio (Aubinet et al., 2008) not accounted for into

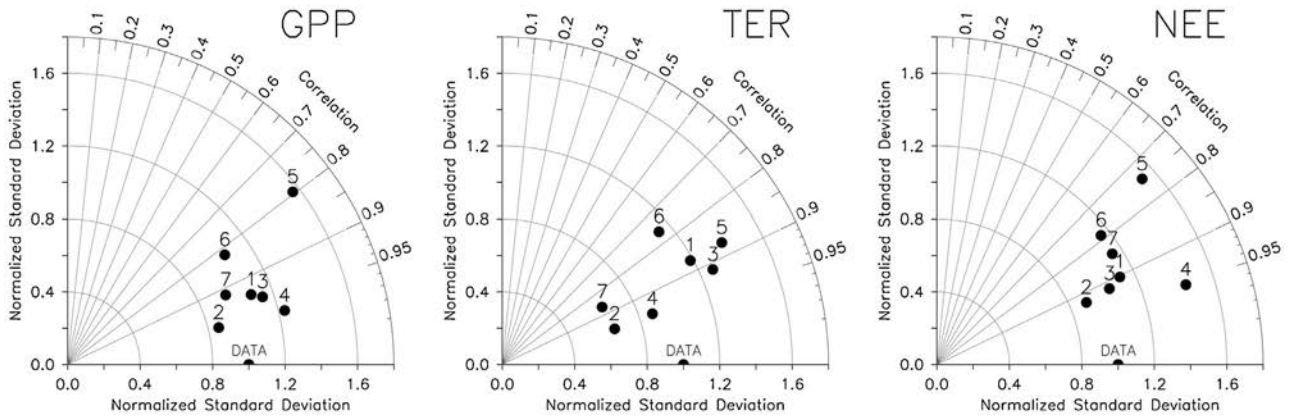


Fig. 4. Taylor diagrams representing model performance for GPP (left panel), TER (middle panel) and NEE (right panel) in a polar coordinate system where the radial coordinate is the normalized standard deviation (NSTD) of the modelled daily fluxes from the observed one and the angular coordinate the correlation between modelled and observation-based fluxes, for each of the seven studied sites (circles): (1) AUR, (2) GEB, (3) GRI, (4) KLI, (5) LAM, (6) LUT and (7) OEN.

the variety-related parameters that STICS transmits to ORCHIDEE. However, observed GPP was positive right after the seeding and right after the harvest, which may suggest the presence of another vegetation type than only wheat in the footprint area (e.g. volunteers) that was ignored in the model set-up. This contribution of non-wheat vegetation cover could explain the misfit for both GPP and TER but only during winter. Alternatively, the TER misfit at OEN could be also explained by an error in simulating HR because the year before wheat was grown, potatoes have been cultivated but never harvested (Ceschia, pers. comm.). It is well possible that the high observed-based TER values are due to the decomposition of the potatoes.

Note also that as observed by Aubinet et al. (2009) and Eugster et al. (2010), there was no significant change in the TER dynamics right after ploughing events (pink vertical lines in TER panels of Fig. 3). The choice in ORCHIDEE-STICS to not account for the effect of soil mechanical disturbance on decomposition processes thus seems consequently appropriate. However, Beziat et al. (2009) noticed that when associated with rainfall events and incorporation of plant residues, ploughing could contribute to important soil respiration increases.

Table 3
Observed and modelled cumulative annual GPP, TER and NEE over the studied one-year period starting on the sowing dates at the seven studied sites and model performance in calculating observed annual budget, expressed as the difference between the observed and simulated cumulative annual flux normalized by the observed flux, the CTRL simulation and the model sensitivity tests.

Flux	Site	Annual Flux ($\text{g C m}^{-2} \text{ yr}^{-1}$)		Model performance (%)						
		OBS ^a	CTRL ^b	CTRL	LOPLANT ^b	HIPLANT ^b	NOFERT ^b	HIFERT ^b	VTA ^b	VTH ^b
GPP	AUR	1123	949	-15	-12	-25	-55	-7	-12	-15
	GEB	1005	851	-15	-17	-17	-35	10	-34	-31
	GRI	1090	1073	-2	2	-8	-41	2	2	-1
	KLI	1179	1233	5	8	-2	-63	11	-2	0
	LAM	1442	1726	20	23	13	-40	20	22	19
	LUT	1355	1423	5	7	112	-49	4	-7	-6
	OEN	1886	1080	-43	-41	-42	-67	-32	-56	-54
TER	AUR	824	973	18	22	11	-50	26	15	13
	GEB	1020	614	-40	-40	-38	-55	-24	-55	-54
	GRI	895	1036	16	20	11	-46	19	3	3
	KLI	1028	921	-10	-7	-14	-67	-5	-22	-20
	LAM	1071	1268	18	22	12	-45	18	17	14
	LUT	904	1233	36	39	35	-45	34	14	16
	OEN	1711	835	-51	-45	-52	-72	-41	-63	-61
NEE	AUR	-298	23	-108	-105	-123	-69	-99	-87	-91
	GEB	15	-236	-1673	-1620	-1473	-1380	-2300	-1507	-1567
	GRI	-194	-37	-81	-79	-98	-15	-76	-2	-18
	KLI	-151	-312	107	113	82	-32	114	138	136
	LAM	-371	-458	23	26	16	-26	25	36	33
	LUT	-451	-190	-58	-56	-52	-58	-55	-50	-50
	OEN	-174	-245	41	-7	56	-17	57	9	16

^a OBS: observations.

^b See Table 2 for simulation's definition.

3.1.4. NEE

Simulating NEE dynamics accurately is more difficult than for GPP or TER, because NEE is the sum of the two opposite fluxes subject to different processes. On the other hand, model errors that impact GPP and TER may partly cancel each other when focusing on NEE. For instance at OEN, the seasonal variations of NEE were relatively well reproduced by the model but not those of GPP and TER individually (Fig. 3). At this site in particular, ORCHIDEE-STICS performed better than the DNDC model at simulating NEE seasonal variations (Dietiker et al., 2010). Over the seven studied sites,

maximal value for NEE was of $4\text{ g C m}^{-2}\text{ d}^{-1}$ (positive value denoting a source of CO_2 to the atmosphere), and minimal NEE was of $-10\text{ g C m}^{-2}\text{ d}^{-1}$ (right column, Fig. 3). Overall, the general seasonal cycle of NEE was similar to the one of GPP (Fig. 3). At most of the sites, the critical period defining large model-data misfit for NEE was the same to those identified for either GPP or TER: At LUT, the critical periods were the same for NEE and GPP; at AUR, KLI, OEN and GEB, the critical periods were the same for NEE and TER; at LAM, the critical periods were the same for NEE, GPP and TER. It

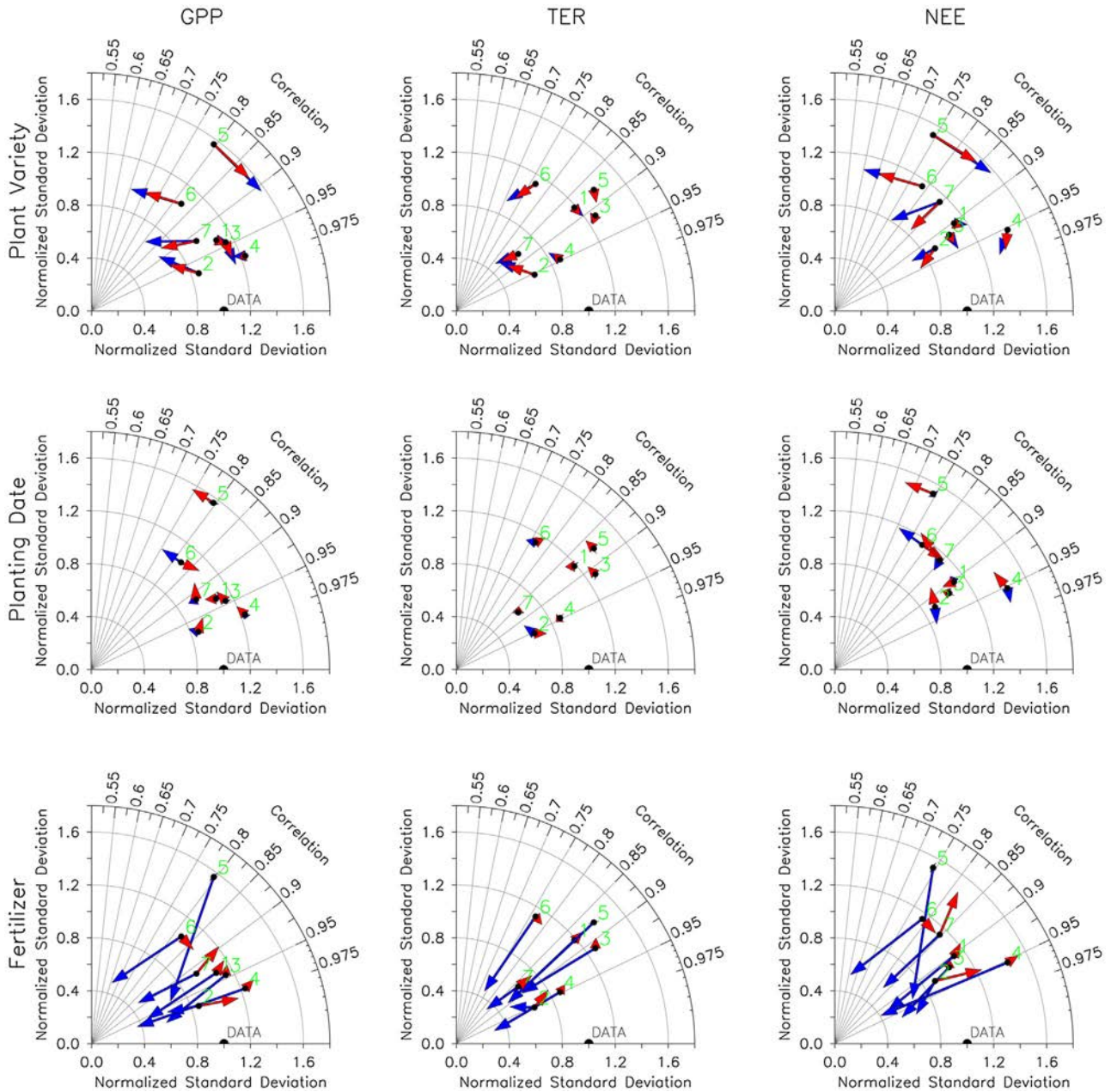


Fig. 5. Taylor diagrams representing model sensitivity to plant variety (top panels), sowing date (middle panels) and fertilizer intensity (bottom panels), for GPP (left panels), TER (middle panels) and NEE (right panels) for each of the seven studied sites (circles): (1) AUR, (2) GEB, (3) GRI, (4) KLI, (5) LAM, (6) LUT and (7) OEN. The start of the arrows corresponds to the CTRL simulation and the end to the sensitivity simulation. Blue arrows indicate model sensitivity tests VTA, LOPLANT and NOFERT, red arrows indicate model sensitivity tests VTH, HIPLANT and HIFERT. (For interpretation of the references to colour in this figure legend, the reader is referred to the web version of this article.)

was only at GRI, that the critical period for NEE differs from those identified for GPP and TER.

The values of the NSTD metrics for daily NEE were as good as those obtained for GPP, and R-values for NEE and TER are similar (see Fig. 4 and Table C1 in Appendix C). Correlation coefficients (R) between simulated and modelled NEE are higher in the present study (mean R=0.75) than those (mean R=0.55) obtained for maize sites by Li et al. (2011) with the same model. R-values are comparable to the values obtained by Sus et al. (2010) with the SPA model over the same set of sites (R=0.83). Root Mean Square Error for NEE varied from 1.2 g C m⁻² d⁻¹ (GEB) to up to 3.1 g C m⁻² d⁻¹ (LAM). The mean RMSE over all sites equalled 1.9 g C m⁻² d⁻¹, which is comparable to the value obtained by Sus et al. (2010) (mean RMSE of 1.5 g C m⁻² d⁻¹) but significantly larger than the values reported by Li et al. (2011) for five maize sites with the ORCHIDEE-STICS model (mean RMSE of 0.9 g C m⁻² d⁻¹)

3.2. Annual budgets

Observed GPP_{cum} ranged from 1005 g C m⁻² yr⁻¹ at GEB to 1886 g C m⁻² yr⁻¹ at OEN (mean value across sites was 1297 g C m⁻² yr⁻¹) (Table 3). ORCHIDEE-STICS performed relatively well in simulating GPP_{cum}. Across all the sites, the RMSE of modelled GPP_{cum} to the observed one equalled 127 g C m⁻² yr⁻¹ or 9.8% of the mean observed value. It is comparable with the uncertainty (100 g C m⁻² yr⁻¹) on annual NEE and its components GPP and TER, associated with measurement and partitioning techniques estimated by Papale et al. (2006), albeit the estimated uncertainty is well below this value at most sites studied by Papale et al. (2006). For comparison, Li et al. (2011) reported EP values for GPP_{cum} varying from 15% to 58%, when simulating maize sites with ORCHIDEE-STICS. In our study, the largest difference was obtained at OEN where ORCHIDEE-STICS underestimated GPP_{cum} by 806 g C m⁻² yr⁻¹ (43%). Interestingly, OEN was also the site where the model/mismatch on the latent heat flux was the largest (see Fig. D1 in Appendix D).

At three over the four sites where AGB was measured, GPP_{cum} was well estimated by ORCHIDEE-STICS (AUR, GRI and KLI) while the model underestimated the maximal AGB value over the growing season. At the fourth site (LAM), modelled GPP was overestimated while the maximal AGB value was well simulated by the model. This tends to indicate either an incorrect modelling of the shoot:root NPP partitioning or an overestimation of the AR term. On this latter issue, Sus et al. (2010) showed that the fraction of GPP respired (the AR term) “is a major control on model sensitivity, as it largely determines the amount of C available for growth”. Based on the work of Amthor (2000b), this fraction is not constant throughout the plant’s life span but changes with crop development.

Similar performances were obtained for the TER_{cum}, although being slightly lower than for GPP_{cum}. Minimal and maximal observed TER_{cum} were 824 g C m⁻² yr⁻¹ (at AUR) and 1711 g C m⁻² yr⁻¹ (at OEN), respectively. Over the seven studied sites, RMSE equalled 152 g C m⁻² yr⁻¹ which corresponds to 14.3% of the mean observed value. This corresponds to a much lower EP value than those reported by Li et al. (2011) for ORCHIDEE-STICS over maize sites (where EP ranges from 31 to 52%). Modelled TER to GPP ratios varied within the same range (from 0.73 to 1.01) as the observations. These values are similar to those cited in previous studies (Suyker et al., 2005; Falge et al., 2002; Gilmanov et al., 2003). However, ORCHIDEE-STICS does not reproduce inter-site variations of the TER to GPP ratio.

Compared to GPP_{cum} or TER_{cum}, the model’s performance at simulating NEE_{cum} was reduced. Overall across the 7 sites, RMSE of NEE_{cum} was 78 g C m⁻² yr⁻¹. Observed NEE_{cum} varied between -451 g C m⁻² yr⁻¹ at LUT (net sink) and 15 g C m⁻² yr⁻¹ (net source)

at GEB. Thus, the RMSE represented 34% of the observed mean value. At AUR, GRI and KLI sites where model/data disagreement for both annual GPP and TER did not exceed 18%, the disagreement for NEE was never less than 80% of the observed value (see Table 3). Although high, the model/data mismatch on NEE_{cum} is reduced compared to former studies. In particular, Sus et al. (2010) calculated over 8 sites, a mean absolute difference between observed and modelled NEE of 134 g C m⁻².

Specific model structural error can explain the lower performance for simulating NEE annual budget as detailed further. NEE can be written as C_{import} - C_{export} + soil C change. All our simulations have been initialized at steady-state and consequently do not account for soil C disequilibrium (Carvalho et al., 2008). This model set-up impacted negatively and much strongly on the model performance at simulating NEE_{cum}, compared to TER_{cum}.

At any site, the model bias on CO₂ fluxes (GPP, TER and NEE) had the same sign during the entire one-month critical period (see Fig. 3 where black and red lines do not cross during the one-month critical period). Consequently, when focusing on cumulative annual fluxes over a crop season, the one-month critical period obtained for seasonal variation was the period that contributed the most to the model bias on an annual basis. Based on this, one may expect to automatically obtain better annual budgets when improving model’s performance in term of seasonal variations. This is especially true because the sign of the difference between modelled and measured fluxes over the one-month critical period or cumulated over a crop season is similar (compare Fig. 3 and Table 3).

3.3. Sensitivity to management parameters

3.3.1. Seasonality

3.3.1.1. Sensitivity to variety parameters. GPP was sensitive to wheat variety parameters used as input of STICS only at 4 sites (LUT, GEB, OEN and LAM, see Fig. 5). This shows that this sensitivity is not systematic and is also dependent on the meteorological conditions observed on-site. Maximum correlation change for GPP equalled 0.17 (~20% at LUT) and change in NSTD never exceeded 0.29 (~30% at OEN). TER was less sensitive to the choice of wheat variety than GPP: maximum correlation and NSTD changes equalled respectively 0.12 and 0.22. Last, NEE performance changes were driven as those of GPP, trajectories being similar both in term of sign and amplitude.

3.3.1.2. Sensitivity to sowing date. In comparison to wheat variety, all fluxes were less sensitive to the varied sowing date (Fig. 5). As already highlighted for the sensitivity to plant variety, GPP and TER fluxes were not equally sensitive to sowing date, the modelled TER fluxes being quasi insensitive to sowing date. At all sites (except LUT), assuming a late sowing date had a bigger impact on CO₂ fluxes than an early one. This asymmetrical response of flux to sowing date is logical since the vegetation onset in STICS is driven by a Growing Degree Days (GDD) function so that seeds accumulate more GDD during the 25 days after the observed sowing date than during the 25 days before. This asymmetrical response to sowing date was also noted by Li et al. (2011) over maize sites. Changes driven by sowing date were mainly obtained along the ‘Correlation axis’ and not that much along the ‘NSTD axis’ of the Taylor diagrams in Fig. 5. This implies that the sowing date modulates the phase of the seasonal cycle but less its amplitude.

3.3.1.3. Sensitivity to fertilization. Of the three studied factors, fertilization was the management driver that impacted the most the three modelled fluxes of GPP, TER and NEE (Fig. 5). Note that we assumed extreme values in the N-fertilization sensitivity tests.

Nevertheless, the sensitivity of the C fluxes to the fertilization rate could be different if considered over a longer period than a year, because nitrogen in the soil adjusts to new N amounts from its initial value to lower values in the NOFERT treatment, or to higher values in the HIFERT treatment. In absence of detailed site history data, we did not investigate the dependency of our sensitivity test results from the initial soil N. In contrary to the sensitivity to plant variety and sowing date, TER was equally sensitive as GPP or NEE to a different fertilization rate. Main change in model performance was obtained for the NSTD metrics: among all C fluxes (GPP, TER and NEE), NSTD change between the CTRL N-fertilization and the no or maximal N-fertilization ranged from 0.15 to 1.03 (25% and 70% of the NSTD obtained for the CTRL simulation, respectively) while the correlation change never exceeded 0.18 (25% change, at LAM). Thus, fertilization modifies more the amplitude of the modelled seasonal cycle of C fluxes than its phase. Last, model performance changes were much bigger under the NOFERT treatment than under the HIFERT one. This clearly shows that the studied sites – as currently managed – are close to the case of non-nutrient limited systems. Nevertheless, no relationship was found between the sensitivity of C fluxes to fertilization and the rate of fertilization applied at each site.

3.3.2. Annual budgets

Compared to the CTRL simulation, the NOFERT treatment was the most sensitive one for GPP_{cum} (Table 3). Under that treatment, the annual GPP value decreased by 40–60%. This is not surprising since fertilization was the treatment that impacted most GPP seasonal variation and especially its amplitude (see NSTD changes in Fig. 5). At some sites where the NSTD changes were significant when changing wheat variety (OEN, GEB and LUT, see Fig. 5), the modelled annual GPP changed by 20%. At other sites (GRIM, KLI, LAM, AUR), the change between wheat varieties never exceeded few percent on modelled GPP. While model performance may differ for TER and GPP at some sites (e.g. AUR, LUT), the difference between CTRL and sensitivity tests was similar for both TER and GPP, at any site. Compared to the results obtained for GPP and TER, annual NEE changes induced by the different sensitivity tests were more complex. Notably, changes of annual NEE were not related to those obtained for Correlation and NSTD when evaluating the model in term of seasonal variations (see Fig. 5 and Table 3). For instance, at LUT, the large NSTD change in the NOFERT treatment did not imply a large impact on annual NEE. On the opposite, at GRI for instance, where no change was observed for correlation nor NSTD under the plant variety treatments, large change was obtained for annual NEE.

4. Conclusions

- Over all sites, between 50% and 90% of the observed seasonal variations of GPP, TER and NEE can be explained by the ORCHIDEE-STICS model (R^2 ranged between 0.5 and 0.9). Many model-data discrepancies in GPP seasonal variations are explained by errors on phenology (LAI development). The one-month critical periods generally differ for GPP and TER, which indicates that there are mechanisms specific to TER, which are incorrectly represented into ORCHIDEE-STICS. This might be the case for the climate response on litter decomposition for instance. Based on the simulations at the seven site-years, the main model bias in seasonal NEE variations can often be explained by a bias in TER.
- On an annual basis, mean deviation does not exceed 10% and 15% of the observed mean value, for GPP and TER respectively. For NEE, the model cannot reproduce annual values, mean deviation corresponding to ~35% of the observed mean value. This clearly shows that more accurate estimates of GPP and TER are required

for estimating NEE annual budgets for wheat fields. This is to relate to other studies (Keenan et al., 2012; Stoy et al., 2013) which clearly show that current terrestrial ecosystem models – with some including crop specificities – fail to reproduce the observed annual means and inter-annual variations of the net CO_2 flux. Underrepresentation of the variability in spring phenology is one of the systematic errors, common to all models used by Keenan et al. (2012) that may explain the biases in modelled NEE annual means. In addition, the effects on soil carbon disequilibrium (related to site history, tillage and to the stabilization of soil organic matter) that were not accounted for in the simulations are probably important processes that determine the long-term soil C change.

- From the sensitivity analysis of the modelled fluxes to three management practices (plant variety, sowing date and fertilization intensity), we clearly find that the fertilization is the one having the largest impact on the model's performance for any flux, both in terms of seasonal variations and annual budgets. However, comparing flux sensitivity to different management parameters is challenging. In our sensitivity analysis, the different management practices were changed one at a time, which prevents to account for the interactions between practices. In addition, Plant variety sensitivity was established qualitatively by using the parameter values of two different varieties, while fertilizer intensity and sowing date parameters were varied quantitatively. Last, the ranges of variability associated to each driver were not comparable: $[-25,+25]$ days compared to the observed value for the sowing date and $[0, \text{optimal supply}]$ for fertilizer intensity. In this respect, it would be of interest to link the ranges of variability to the uncertainties associated to these management practices at regional scale.

Acknowledgement

This study was supported by the European Commission (CarboEurope Integrated Project, EU FP6 505572).

Appendix A.

The development stages considered for the phenology in STICS are the emergence (LEV), the maximal leaf growth (end of juvenile phase, AMF), the maximal leaf area index (LAX), the first day of decrease of LAI (SEN), and the day when LAI equals 0 (LAN). In addition, for the grain filling, we consider the beginning of grain filling (DRP) and the physiological maturity stage (MAT)

The thermal requirements between two consecutive stages differ for the different wheat varieties considered in this study. Their values as well as those of two variety-specific parameters are given in Table A1.

Appendix B.

See Table B1.

Appendix C.

See Table C1.

Appendix D.

See Fig. D1.

Table A1
Development stages used in STICS and thermal requirements for the different wheat varieties used in this study.

Variety/Parameter ^a	jvc	stlevamf	stamflax	stlaxsen	stsenlan	stlevdrp	stdrpmat	pgrainmaxi
Arminda	50	260	401	251	588	812	760	0.042
Thalent	33	203	294	287	588	684	760	0.036
Thésée	33	237	294	287	588	706	760	0.049

^a jvc: the number of vernalizing days required (days); stlevamf: the duration between LEV and AMF (degree-day); stamflax: the duration between AMF and LAX (degree-day); stlaxsen: the duration between LAX and SEN (degree-day); stsenlan: the duration between SEN and LAN (degree-day); stlevdrp: the duration between LEV and DRP (degree-day); stdrpmat: the duration between DRP and MAT (degree-day); pgrainmaxi: the maximum dry weight of one grain (g).

Table B1
Instrumental characteristics at the seven monitored sites.

Site id	Meas. height (m)	Analyzer	Analyzer model	Anemometer model	Precipitation sensor	Global radiation	Air temperature	Atmospheric pressure	Relative humidity	Wind horizontal speed
AUR	2.8	open	LI-COR LI-7500	Campblel, Cs3	Environmental Measurements, ARG100	Kipp & Zonen, CNR1	Vaisala, HMP35A	Delta-T, BS4	Vaisala, HMP35A	Young, 05103
GEB.	3	closed	LI-COR LI-6262 and LI-7000	Solent, R3	Thies, tipping bucket rain gauge	Kipp & Zonen, CM14	Vaisala, HMP45D	Vaisala, PTB101B	Vaisala, HMP45D	Vector, A100R
GRI	3	open	LI-COR LI-7500	Gill, R3	Unknown	Kipp & Zonen, CM6B	unknown	unknown	unknown	unknown
KLI	3.5	closed	LI-COR LI-7000	Solent, R3	PLUVIO (OTT)	Kipp & Zonen, CNR1	Vaisala, HMP45	unknown	Vaisala, HMP45	Solent, R3
LAM	3.65	open	LI-COR LI-7500	Campblel, Cs3	Environmental Measurements, ARG100	Kipp & Zonen, CNR1	Vaisala, HMP35A	Delta-T, BS4	Vaisala, HMP35A	Gill, WindSonic
LUT	2	open	LI-COR LI-7500	Gill, R3-50	Environmental Measurements, ARG100	Kipp & Zonen, CM21	Vaisala, HMP45A	Vaisala, PTB101C	Vaisala, HMP45A	Gill, R3-50
OEN	1.6	open	LI-COR LI-7500	Solent, R50	Young	Kipp & Zonen, CNR1	Rotronic, MP101A	LI-7500	Rotronic, MP101A	Vector

Table C1
RMSE ($\text{g C m}^{-2} \text{ d}^{-1}$), R and bias ($\text{g C m}^{-2} \text{ d}^{-1}$) between the measured and modelled daily variations of GPP, TER and NEE fluxes at the seven studied sites.

	Metric/Site	AUR	GEB	GRI	KLI	LAM	LUT	OEN
GPP	RMSE	1.57	1.08	1.68	1.71	4.33	3.12	2.97
	R	0.93	0.97	0.94	0.97	0.80	0.82	0.92
	Bias	-0.48	-0.42	-0.05	0.15	0.78	0.19	-2.21
TER	RMSE	0.96	1.38	0.97	0.89	1.46	1.74	2.94
	R	0.88	0.95	0.91	0.94	0.87	0.76	0.87
	Bias	0.41	-1.11	0.39	-0.29	0.54	0.90	-2.40
NEE	RMSE	1.61	1.16	1.46	1.64	3.10	2.45	1.65
	R	0.90	0.92	0.92	0.95	0.74	0.79	0.85
	Bias	0.88	-0.69	0.43	-0.44	-0.24	0.72	-0.19

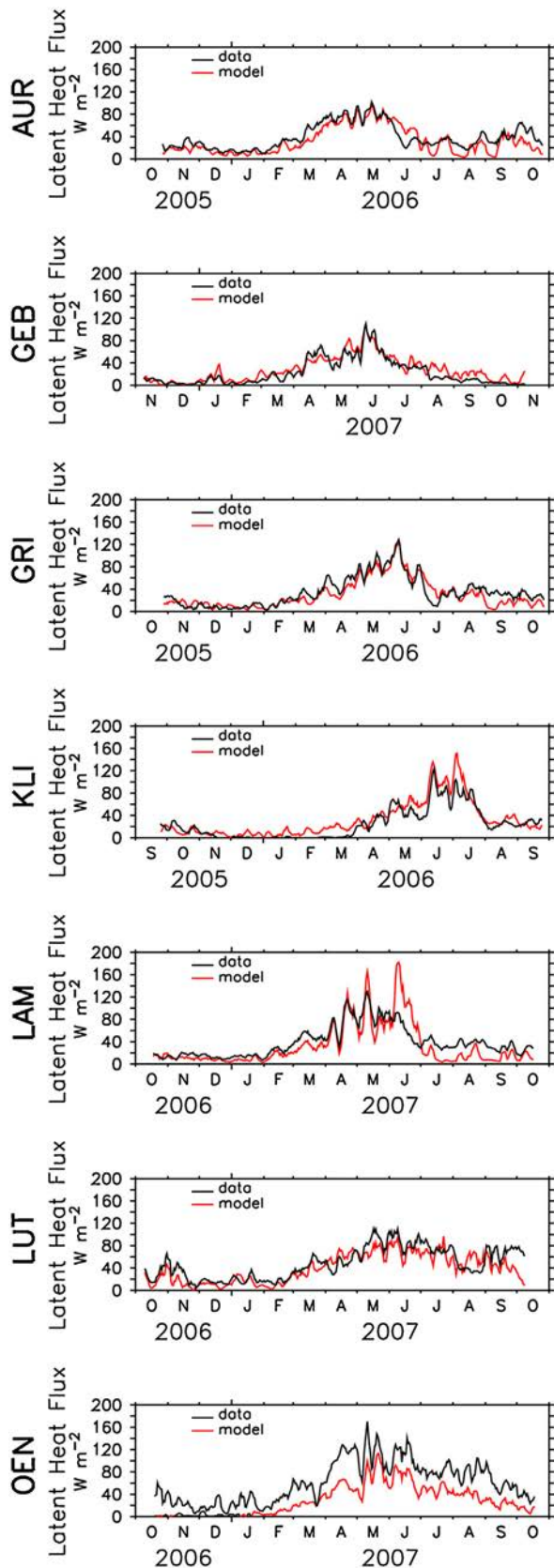


Fig. D1. Observation-based (black) and modelled (red) daily variations (five-days running mean) of the latent heat flux expressed as W m^{-2} for the seven studied sites over the one-year period starting on the sowing dates. (For interpretation of the references to colour in this figure legend, the reader is referred to the web version of this article.)

References

- Ammann, C., Spirig, C., Leifeld, J., Neftel, A., 2009. Assessment of the nitrogen and carbon budget of two managed temperate grassland fields. *Agric. Ecosyst. Environ.* 133, 150–162.
- Amthor, J.S., 2000a. Direct effect of elevated CO_2 on nocturnal in situ leaf respiration in nine temperate deciduous tree species is small. *Tree Physiol.* 20, 139–144.
- Amthor, J., 2000b. The McCree–de Wit–Penning de Vries–Thornley respiration paradigms: 30 years later. *Ann. Bot.* 86, 1–20. doi:<http://dx.doi.org/10.1006/anbo.2000.1175>.
- Anderson, D.E., Verma, S.B., 1986. Carbon-dioxide, water-vapor and sensible heat exchanges of a grain-sorghum canopy. *Bound. Layer Meteorol.* 34, 317–331.
- Anderson, D.E., Verma, S.B., Rosenberg, N.J., 1984. Eddy-correlation measurements of CO_2 , latent-heat, and sensible heat fluxes over a crop surface. *Bound. Layer Meteorol.* 29, 263–272.
- Aubinet, M., Grelle, A., Ibrom, A., Rannik, U., Moncrieff, J., Foken, T., Kowalski, A.S., Martin, P.H., Berbigier, P., Bernhofer, C., Clement, R., Elbers, J., Granier, A., Grunwald, T., Morgenstern, K., Pilegaard, K., Rebmann, C., Snijders, W., Valentini, R., Vesala, T., 2000. Estimates of the annual net carbon and water exchange of forests: the EUROFLUX methodology. *Adv. Ecol. Res.* 30, 113–175.
- Aubinet, M., Moureaux, C., Bodson, B., Dufranne, D., Heinesch, B., Suleau, M., Vancutsem, F., Vilret, A., 2009. Carbon sequestration by a crop over a 4-year sugar beet/winter wheat/seed potato/winter wheat rotation cycle. *Agric. For. Meteorol.* 149, 407–418.
- Baldocchi, D.D., 2003. Assessing the eddy covariance technique for evaluating carbon dioxide exchange rates of ecosystems: past, present and future. *Glob. Change Biol.* 9, 479–492.
- Ball, J.T., Woodrow, I.E., Berry, J.A., 1987. A model predicting stomatal conductance and its contribution to the control of photosynthesis under different environmental conditions. *Progress in Photosynthesis Research*. Springer, Netherlands (pp. 221–224).
- Bellamy, P.H., Loveland, P.J., Bradley, R.I., Lark, R.M., Kirk, G.J.D., 2005. Carbon losses from all soils across England and Wales 1978–2003. *Nature* 437, 245–248.
- Beziat, P., Ceschia, E., Dedieu, G., 2009. Carbon balance of a three crop succession over two cropland sites in South West France. *Agric. For. Meteorol.* 149, 1628–1645.
- Bilionis, I., Drewniak, B.A., Constantinescu, E.M., 2015. Crop physiology calibration in the CLM. *Geosci. Model Dev.* 8, 1071–1083.
- Bondeau, A., Smith, P.C., Zaehle, S., Schaphoff, S., Lucht, W., Cramer, W., Gerten, D., Lotze-Campen, H., Mueller, C., Reichstein, M., Smith, B., 2007. Modelling the role of agriculture for the 20th century global terrestrial carbon balance. *Glob. Change Biol.* 13, 679–706.
- Brisson, N., Mary, B., Ripoche, D., Jeuffroy, M.H., Ruget, F., Nicoullaud, B., Gate, P., Devienne-Barret, F., Antonioletti, R., Durr, C., Richard, G., Beaudoin, N., Recous, S., Tayot, X., Plenet, D., Cellier, P., Machet, J.M., Meynard, J.M., Delecolle, R., 1998. STICS: a generic model for the simulation of crops and their water and nitrogen balances. I. Theory and parameterization applied to wheat and corn. *Agronomie* 18, 311–346.
- Brisson, N., Ruget, F., Gate, P., Lorgeau, J., Nicoullaud, B., Tayot, X., Plenet, D., Jeuffroy, M.H., Bouthier, A., Ripoche, D., Mary, B., Justes, E., 2002. STICS: a generic model for simulating crops and their water and nitrogen balances. II. Model validation for wheat and maize. *Agronomie* 22, 69–92.
- Brisson, N., Gary, C., Justes, E., Roche, R., Mary, B., Ripoche, D., Zimmer, D., Sierra, J., Bertuzzi, P., Burger, P., Bussiere, F., Cabidoche, Y.M., Cellier, P., Debaeke, P., Gaudillere, J.P., Henault, C., Maraux, F., Seguin, B., Sinoquet, H., 2003. An overview of the crop model STICS. *Eur. J. Agron.* 18, 309–332.
- Brisson, N., Launay, M., Mary, B., Beaudoin, N., 2008. **Conceptual Basis, Formalizations and Parameterization of the Stics Crop Model.** *Quae ed.*
- Canadell, J.G., Ciais, P., Gurney, K., Le Quéré, C., Piao, S., Raupach, M.R., Sabine, C.L., 2011. An international effort to quantify regional carbon fluxes. *Eos Trans. AGU* 92 (10), 81.
- Cannell, M.G.R., Thornley, J.H.M., 2000. Modelling the components of plant respiration: some guiding principles. *Ann. Bot.* 85, 45–54.
- Carvalho, N., Reichstein, M., Seixas, J., Collatz, G.J., Pereira, J.S., Berbigier, P., Carrara, A., Granier, A., Montagnani, L., Papale, D., Rambal, S., Sanz, M.J., Valentini, R., 2008. Implications of the carbon cycle steady state assumption for biogeochemical modeling performance and inverse parameter retrieval. *Glob. Biogeochem. Cycles* 22.
- Ceschia, E., Béziat, P., Dejoux, J.F., Aubinet, M., Bernhofer, C., Bodson, B., Buchmann, N., Carrara, A., Cellier, P., Di Tommasi, P., Elbers, J.A., 2010. Management effects on net ecosystem carbon and GHG budgets at European crop sites. *Agric. Ecosyst. Environ.* 139 (3), 363–383.
- Chapin, F.S., Woodwell, G.M., Randerson, J.T., Rastetter, E.B., Lovett, G.M., Baldocchi, D.D., Clark, D.A., Harmon, M.E., Schimel, D.S., Valentini, R., Wirth, C., Aber, J.D., Cole, J.J., Goulden, M.L., Harden, J.W., Heimann, M., Howarth, R.W., Matson, P.A., McGuire, A.D., Melillo, J.M., Mooney, H.A., Neff, J.C., Houghton, R.A., Pace, M.L., Ryan, M.G., Running, S.W., Sala, O.E., Schlesinger, W.H., Schulze, E.-D., 2006. Reconciling carbon-cycle concepts, terminology, and methods. *Ecosystems* 9, 1041–1050. doi:<http://dx.doi.org/10.1007/s10021-005-0105-7>.
- Ciais, P., Wattenbach, M., Vuichard, N., Smith, P., Piao, S.L., Don, A., Luysaert, S., Janssens, I.A., Bondeau, A., Dechow, R., Leip, A., Smith, P.C., Beer, C., van der Werf, G.R., Gervois, S., Van Oost, K., Tomelleri, E., Freibauer, A., Schulze, E.D., Team, C.S., 2010. The European carbon balance. Part 2: croplands. *Glob. Change Biol.* 16, 1409–1428.

- Collatz, G., Ribas-Carbo, M., Berry, J., 1992. Coupled photosynthesis-stomatal conductance model for leaves of C4 plants. *Aust. J. Plant Physiol.* 19, 519–538.
- de Noblet-Ducoudre, N., Gervois, S., Ciais, P., Viovy, N., Brisson, N., Seguin, B., Perrier, A., 2004. Coupling the soil-vegetation-atmosphere-transfer scheme ORCHIDEE to the agronomy model STICS to study the influence of croplands on the European carbon and water budgets. *Agronomie* 24, 397–407.
- Desai, A.R., Richardson, A.D., Moffat, A.M., Kattge, J., Hollinger, D.Y., Barr, A., Falge, E., Noormets, A., Papale, D., Reichstein, M., Stauch, V.J., 2008. Cross-site evaluation of eddy covariance GPP and RE decomposition techniques. *Agric. For. Meteorol.* 148, 821–838.
- Desjardins, R.L., Lemon, E.R., 1971. CO₂ flux measurements by eddy correlation technique. *Bull. Am. Meteorol. Soc.* 52, 309.
- Desjardins, R.L., Lemon, E.R., 1974. Limitations of an eddy-correlation technique for the determination of the carbon dioxide and sensible heat fluxes. *Bound. Layer Meteorol.* 5, 475–488.
- Desjardins, R.L., Buckley, D.J., Stomour, G., 1984. Eddy flux measurements of CO₂ above corn using a microcomputer system. *Agric. For. Meteorol.* 32, 257–265.
- Dietiker, D., Buchmann, N., Eugster, W., 2010. Testing the ability of the DNDC model to predict CO₂ and water vapour fluxes of a Swiss cropland site. *Agric. Ecosyst. Environ.* 139, 396–401. doi:http://dx.doi.org/10.1016/j.agee.2010.09.002.
- Dolman, A.J., Noilhan, J., Durand, P., Sarraz, C., Brut, A., Pignat, B., Butet, A., Jarosz, N., Brunet, Y., Loustau, D., Lamaud, E., Tolk, L., Ronda, R., Miglietta, F., Gioli, B., Magliulo, V., Esposito, M., Gerbig, C., Korner, S., Glademard, R., Ramonet, M., Ciais, P., Neininger, B., Hutjes, R.W.A., Elbers, J.A., Macatangay, R., Schrems, O., Perez-Landa, G., Sanz, M.J., Scholz, Y., Facon, G., Ceschia, E., Beziat, P., 2006. The CarboEurope regional experiment strategy. *Bull. Am. Meteorol. Soc.* 87, 1367–1379.
- Ellis, E.C., Ramankutty, N., 2008. Putting people in the map: anthropogenic biomes of the world. *Front. Ecol. Environ.* 6, 439–447.
- Enting, I.G., Rayner, P.J., Ciais, P., 2012. Carbon cycle uncertainty in regional carbon cycle assessment and processes (RECCAP). *Biogeosciences* 9, 2889–2904.
- Eugster, W., Moffat, A.M., Ceschia, E., Aubinet, M., Ammann, C., Osborne, B., Davis, P. A., Smith, P., Jacobs, C., Moors, E., Le Dantec, V., Beziat, P., Saunders, M., Jans, W., Gruenwald, T., Rebmann, C., Kutsch, W.L., Czerny, R., Janous, D., Moureaux, C., Dufranne, D., Carrara, A., Magliulo, V., Di Tommasi, P., Olesen, J.E., Schelde, K., Olioso, A., Bernhofer, C., Cellier, P., Larmanou, E., Loubet, B., Wattenbach, M., Marloie, O., Sanz, M.-J., Sogaard, H., Buchmann, N., 2010. Management effects on European cropland respiration. *Agric. Ecosyst. Environ.* 139, 346–362.
- Falge, E., Baldocchi, D., Tenhunen, J., Aubinet, M., Bakwin, P., Berbigier, P., Bernhofer, C., Burba, G., Clement, R., Davis, K.J., Elbers, J.A., Goldstein, A.H., Grelle, A., Granier, A., Guomundsson, J., Hollinger, D., Kowalski, A.S., Katul, G., Law, B.E., Malhi, Y., Meyers, T., Monson, R.K., Munger, J.W., Oechel, W., Paw, K.F.T., Pilegaard, K., Rannik, U., Rebmann, C., Suyker, A., Valentini, R., Wilson, K., Wofsy, S., 2002. Seasonality of ecosystem respiration and gross primary production as derived from FLUXNET measurements. *Agric. For. Meteorol.* 113, 53–74.
- Farquhar, G., von Caemmerer, S., Berry, J., 1980. A biochemical model of photosynthesis CO₂ fixation in leaves of C3 species. *Planta* 149, 78–90.
- Gervois, S., de Noblet-Ducoudre, N., Viovy, N., Ciais, P., Brisson, N., Seguin, B., Perrier, A., 2004. Including croplands in a global biosphere model: methodology and evaluation at specific sites. *Earth Interact.* 8.
- Gervois, S., Ciais, P., de Noblet-Ducoudre, N., Brisson, N., Vuichard, N., Viovy, N., 2008. Carbon and water balance of European croplands throughout the 20th century. *Global Biogeochem. Cycles* 22.
- Gilmanov, T.G., Verma, S.B., Sims, P.L., Meyers, T.P., Bradford, J.A., Burba, G.G., Suyker, A.E., 2003. Gross primary production and light response parameters of four Southern Plains ecosystems estimated using long-term CO₂-flux tower measurements. *Glob. Biogeochem. Cycles* 17.
- Huntzinger, D.N., Post, W.M., Wei, Y., Michalak, A.M., West, T.O., Jacobson, A.R., Baker, I.T., Chen, J.M., Davis, K.J., Hayes, D.J., Hoffman, F.M., Jain, A.K., Liu, S., McGuire, A.D., Neilson, R.P., Potter, C., Poulter, B., Price, D., Raczka, B.M., Tian, H., Thornton, P., Tomelleri, E., Viovy, N., Xiao, J., Yuan, W., Zeng, N., Zhao, M., Cook, R., 2012. North American Carbon Program (NACP) regional interim synthesis: terrestrial biospheric model intercomparison. *Ecol. Model.* 232, 144–157.
- Jamagne, M., Bêtrémieux, R., Bégon, J.C., Mori, A., 1977. Quelques données sur la variabilité dans le milieu naturel de la réserve en eau des sols. *Bulletin Technique d'Information du Ministère de l'Agriculture* 324–325, 119–157.
- Keenan, T.F., Baker, I., Barr, A., Ciais, P., Davis, K., Dietze, M., Dragoni, D., Gough, C.M., Grant, R., Hollinger, D., Hufkens, K., Poulter, B., McCaughy, H., Raczka, B., Ryu, Y., Schaefer, K., Tian, H., Verbbeeck, H., Zhao, M., Richardson, A.D., 2012. Terrestrial biosphere model performance for inter-annual variability of land-atmosphere CO₂ exchange. *Glob. Change Biol.* 18, 1971–1987. doi:http://dx.doi.org/10.1111/j.1365-2486.2012.02678.x.
- Kindler, R., Siemens, J., Kaiser, K., Walmsley, D.C., Bernhofer, C., Buchmann, N., Cellier, P., Eugster, W., Gleixner, G., Grunwald, T., Heim, A., Ibram, A., Jones, S.K., Jones, M., Klumpp, K., Kutsch, W., Larsen, S., Lehuger, S., Loubet, B., McKenzie, R., Moors, E., Osborne, B., Pilegaard, K., Rebmann, C., Saunders, M., Schmidt, M. W.I., Schruppf, M., Seyferth, J., Skiba, U., Soussana, J.-F., Sutton, M.A., Tefs, C., Vowinckel, B., Zeeman, M.J., Kaupenjohann, M., 2011. Dissolved carbon leaching from soil is a crucial component of the net ecosystem carbon balance. *Glob. Change Biol.* 17, 1167–1185.
- Kobayashi, K., Salam, M.U., 2000. Comparing simulated and measured values using mean squared deviation and its components. *Agron. J.* 92, 345–352.
- Krinner, G., Viovy, N., de Noblet-Ducoudre, N., Ogee, J., Polcher, J., Friedlingstein, P., Ciais, P., Sitch, S., Prentice, I.C., 2005. A dynamic global vegetation model for studies of the coupled atmosphere-biosphere system. *Glob. Biogeochem. Cycles* 19.
- Kutsch, W.L., Aubinet, M., Buchmann, N., Smith, P., Osborne, B., Eugster, W., Wattenbach, M., Schruppf, M., Schulze, E.D., Tomelleri, E., Ceschia, E., Bernhofer, C., Beziat, P., Carrara, A., Di Tommasi, P., Gruenwald, T., Jones, M., Magliulo, V., Marloie, O., Moureaux, C., Olioso, A., Sanz, M.J., Saunders, M., Sogaard, H., Ziegler, W., 2010. The net biome production of full crop rotations in Europe. *Agric. Ecosyst. Environ.* 139, 336–345.
- Lasslop, G., Reichstein, M., Papale, D., Richardson, A.D., Arneeth, A., Barr, A., Stoy, P., Wohlfahrt, G., 2010. Separation of net ecosystem exchange into assimilation and respiration using a light response curve approach: critical issues and global evaluation. *Glob. Change Biol.* 16, 187–208.
- Levis, S., Bonan, G.B., Kluzek, E., Thornton, P.E., Jones, A., Sacks, W.J., Kucharik, C.J., 2012. Interactive crop management in the Community Earth System Model (CESM1): seasonal influences on land-atmosphere fluxes. *J. Clim.* 25, 4839–4859.
- Li, L., Vuichard, N., Viovy, N., Ciais, P., Wang, T., Ceschia, E., Jans, W., Wattenbach, M., Beziat, P., Gruenwald, T., Lehuger, S., Bernhofer, C., 2011. Importance of crop varieties and management practices: evaluation of a process-based model for simulating CO₂ and H₂O fluxes at five European maize (*Zea mays* L.) sites. *Biogeosciences* 8, 1721–1736.
- Lloyd, J., Taylor, J.A., 1994. On the temperature-dependence of soil respiration. *Funct. Ecol.* 8, 315–323.
- Lokupitiya, E., Denning, S., Paustian, K., Baker, I., Schaefer, K., Verma, S., Meyers, T., Bernacchi, C.J., Suyker, A., Fischer, M., 2009. Incorporation of crop phenology in Simple Biosphere Model (SiBcrop) to improve land-atmosphere carbon exchanges from croplands. *Biogeosciences* 6, 969–986.
- Loubet, B., Laville, P., Lehuger, S., Larmanou, E., Flechard, C., Mascher, N., Genemont, S., Roche, R., Ferrara, R.M., Stella, P., Personne, E., Durand, B., Decuq, C., Flura, D., Masson, S., Fanucci, O., Rampon, J.-N., Siemens, J., Kindler, R., Gabrielle, B., Schruppf, M., Cellier, P., 2011. Carbon, nitrogen and greenhouse gases budgets over a four years crop rotation in northern France. *Plant Soil* 343, 109–137.
- Loubet, B., Cellier, P., Flechard, C., Zurfluh, O., Irvine, M., Lamaud, E., Stella, P., Roche, R., Durand, B., Flura, D., Masson, S., Laville, P., Garrigou, D., Personne, E., Chelle, M., Castell, J.-F., 2013. Investigating discrepancies in heat, CO₂ fluxes and O₃ deposition velocity over maize as measured by the eddy-covariance and the aerodynamic gradient methods. *Agric. For. Meteorol.* 169, 35–50.
- Ma, S., Churkina, G., Wieland, R., Gessler, A., 2011. Optimization and evaluation of the ANTHRO-BGC model for winter crops in Europe. *Ecol. Model.* 222, 3662–3679.
- Monsi, M., Sæki, T., 1953. æber den Lichtfaktor in den Pflanzengesellschaften und seine Bedeutung für die Stoffproduktion. *Jpn. J. Bot.* 14, 22–52.
- Moors, E.J., Jacobs, C., Jans, W., Supit, I., Kutsch, W.L., Bernhofer, C., Beziat, P., Buchmann, N., Carrara, A., Ceschia, E., Elbers, J., Eugster, W., Kruijt, B., Loubet, B., Magliulo, E., Moureaux, C., Olioso, A., Saunders, M., Soegaard, H., 2010. Variability in carbon exchange of European croplands. *Agric. Ecosyst. Environ.* 139, 325–335.
- Ohtaki, E., 1984. Application of an infrared carbon-dioxide and humidity instrument to studies of turbulent transport. *Bound. Layer Meteorol.* 29, 85–107.
- Papale, D., Reichstein, M., Aubinet, M., Canfora, E., Bernhofer, C., Kutsch, W., Longdoz, B., Rambal, S., Valentini, R., Vesala, T., Yakir, D., 2006. Towards a standardized processing of net ecosystem exchange measured with eddy covariance technique: algorithms and uncertainty estimation. *Biogeosciences* 3, 571–583.
- Pape, L., Ammann, C., Nyfeler-Brunner, A., Spirig, C., Hens, K., Meixner, F.X., 2009. An automated dynamic chamber system for surface exchange measurement of non-reactive and reactive trace gases of grassland ecosystems. *Biogeosciences* 6, 405–429.
- Parton, W., Stewart, J., Cole, C., 1988. Dynamics of C, N, P, and S in grassland soil: a model. *Biogeochemistry* 5, 109–131.
- Reichstein, M., Falge, E., Baldocchi, D., Papale, D., Aubinet, M., Berbigier, P., Bernhofer, C., Buchmann, N., Gilmanov, T., Granier, A., Grunwald, T., Havrankova, K., Ilvesniemi, H., Janous, D., Knohl, A., Laurila, T., Lohila, A., Loustau, D., Matteucci, G., Meyers, T., Miglietta, F., Ourival, J.M., Pumpanen, J., Rambal, S., Rotenberg, E., Sanz, M., Tenhunen, J., Seufert, G., Vaccari, F., Vesala, T., Yakir, D., Valentini, R., 2005. On the separation of net ecosystem exchange into assimilation and ecosystem respiration: review and improved algorithm. *Glob. Change Biol.* 11, 1424–1439.
- Running, S.W., Baldocchi, D.D., Turner, D.P., Gower, S.T., Bakwin, P.S., Hibbard, K.A., 1999. A global terrestrial monitoring network integrating tower fluxes, flask sampling, ecosystem modeling and EOS satellite data. *Remote Sens. Environ.* 70, 108–127.
- Schulze, E.D., Luuyssaert, S., Ciais, P., Freibauer, A., Janssens, I.A., Soussana, J.F., Smith, P., Grace, J., Levin, I., Thiruchittampalam, B., Heimann, M., Dolman, A.J., Valentini, R., Bousquet, P., Peylin, P., Peters, W., Roedenbeck, C., Etiope, G., Vuichard, N., Wattenbach, M., Nabuurs, G.J., Poussi, Z., Nieschulze, J., Gash, J.H., CarboEurope, T., 2009. Importance of methane and nitrous oxide for Europe's terrestrial greenhouse-gas balance. *Nat. Geosci.* 2, 842–850.
- Smith, P., Chapman, S.J., Scott, W.A., Black, H.I.J., Wattenbach, M., Milne, R., Campbell, C.D., Lilly, A., Ostle, N., Levy, P.E., Lumsdon, D.G., Millard, P., Towers, W., Zaehle, S., Smith, J.U., 2007. Climate change cannot be entirely responsible for soil carbon loss observed in England and Wales, 1978–2003. *Glob. Change Biol.* 13, 2605–2609.
- Smith, P.C., De Noblet-Ducoudre, N., Ciais, P., Peylin, P., Viovy, N., Meurdesoif, Y., Bondeau, A., 2010a. European-wide simulations of croplands using an improved

- terrestrial biosphere model: phenology and productivity. *J. Geophys. Res. Biogeosci.* 115.
- Smith, P.C., Ciais, P., Peylin, P., De Noblet-Ducoudre, N., Viovy, N., Meurdesoif, Y., Bondeau, A., 2010b. European-wide simulations of croplands using an improved terrestrial biosphere model. 2. Interannual yields and anomalous CO₂ fluxes in 2003. *J. Geophys. Res. Biogeosci.* 115.
- Stoy, P.C., Dietze, M.C., Richardson, A.D., Vargas, R., Barr, A.G., Anderson, R.S., Arain, M.A., Baker, I.T., Black, T.A., Chen, J.M., Cook, R.B., Gough, C.M., Grant, R.F., Hollinger, D.Y., Izaurrealde, R.C., Kucharik, C.J., Lafleur, P., Law, B.E., Liu, S., Lokupitiya, E., Luo, Y., Munger, J.W., Peng, C., Poulter, B., Price, D.T., Ricciuto, D. M., Riley, W.J., Sahoo, A.K., Schaefer, K., Schwalm, C.R., Tian, H., Verbeeck, H., Weng, E., 2013. Evaluating the agreement between measurements and models of net ecosystem exchange at different times and timescales using wavelet coherence: an example using data from the North American Carbon Program Site-Level Interim Synthesis. *Biogeosciences* 10, 6893–6909. doi:<http://dx.doi.org/10.5194/bg-10-6893-2013>.
- Sus, O., Williams, M., Bernhofer, C., Béziat, P., Buchmann, N., Ceschia, E., Doherty, R., Eugster, W., Grünwald, T., Kutsch, W., Smith, P., Wattenbach, M., 2010. A linked carbon cycle and crop developmental model: description and evaluation against measurements of carbon fluxes and carbon stocks at several European agricultural sites. *Agric. Ecosyst. Environ.* 139, 402–418. doi:<http://dx.doi.org/10.1016/j.agee.2010.06.012>.
- Suyker, A.E., Verma, S.B., Burba, G.G., Arkebauer, T.J., 2005. Gross primary production and ecosystem respiration of irrigated maize and irrigated soybean during a growing season. *Agric. For. Meteorol.* 131, 180–190.
- Taylor, K.E., 2001. Summarizing multiple aspects of model performance in a single diagram. *J. Geophys. Res. Atmos.* 106, 7183–7192.
- Thornley, J.H.M., Cannell, M.G.R., 2000. Modelling the components of plant respiration: representation and realism. *Ann. Bot.* 85, 55–67.
- Valade, A., Vuichard, N., Ciais, P., Ruget, F., Viovy, N., Gabrielle, B., Huth, N., Martine, J.-F., 2014. ORCHIDEE-STICS, a process-based model of sugarcane biomass production: calibration of model parameters governing phenology. *Glob. Change Biol. Bioenergy* 6, 606–620.
- Valentini, R., Matteucci, G., Dolman, A.J., Schulze, E.D., Rebmann, C., Moors, E.J., Granier, A., Gross, P., Jensen, N.O., Pilegaard, K., Lindroth, A., Grelle, A., Bernhofer, C., Grunwald, T., Aubinet, M., Ceulemans, R., Kowalski, A.S., Vesala, T., Rannik, U., Berbigier, P., Loustau, D., Guomundsson, J., Thorgeirsson, H., Ibrom, A., Morgenstern, K., Clement, R., Moncrieff, J., Montagnani, L., Minerbi, S., Jarvis, P. G., 2000. Respiration as the main determinant of carbon balance in European forests. *Nature* 404, 861–865.
- Van den Hoof, C., Hanert, E., Vidale, P.L., 2011. Simulating dynamic crop growth with an adapted land surface model—JULES-SUCROS: model development and validation. *Agric. For. Meteorol.* 151, 137–153.
- Vuichard, N., Ciais, P., Beletti, L., Smith, P., Valentini, R., 2008. Carbon sequestration due to the abandonment of agriculture in the former USSR since 1990. *Glob. Biogeochem. Cycles* 22.
- Webb, E.K., Pearman, G., Leuning, R., 1980. Correction of flux measurements for density effects due to heat and water vapour transfer. *Q. J. R. Meteorol. Soc.* 106, 85–100.